

A Morphometric Study of the Lungs of Different Sized Bats: Correlations between Structure and Function of the Chiropteran Lung

John N. Maina, Steven P. Thomas and Dallas M. Hyde

Phil. Trans. R. Soc. Lond. B 1991 **333**, 31-50
doi: 10.1098/rstb.1991.0059

Email alerting service

Receive free email alerts when new articles cite this article - sign up in the box at the top right-hand corner of the article or click [here](#)

To subscribe to *Phil. Trans. R. Soc. Lond. B* go to: <http://rstb.royalsocietypublishing.org/subscriptions>

A morphometric study of the lungs of different sized bats: correlations between structure and function of the chiropteran lung

JOHN N. MAINA¹, STEVEN P. THOMAS² AND DALLAS M. HYDE³

¹ Department of Veterinary Anatomy, University of Nairobi, P.O. Box 30197, Nairobi, Kenya

² Department of Biological Sciences, Duquesne University, Pittsburgh, Pennsylvania 15282, U.S.A.

³ Department of Anatomy, School of Veterinary Medicine, University of California, Davis, California 95616, U.S.A.

CONTENTS

	PAGE
1. Introduction	32
2. Materials and methods	32
(a) Light microscopy	33
(b) Electron microscopy	33
3. Results	33
4. Discussion	35
(a) Evolutionary background	35
(b) Energetic requirements of flight	35
(c) Morphological data of bat lungs and its relation to $\dot{V}_{O_{2max}}$ and size	35
(d) Allometric comparisons of bat, bird and non-flying mammal lung: morphological characteristics and their relations to $\dot{V}_{O_{2max}}$	44
5. References	49

SUMMARY

1. The lungs of four species of bats, *Phyllostomus hastatus* (PH, mean body mass, 98 g), *Pteropus lylei* (PL, 456 g), *Pteropus alecto* (PA, 667 g), and *Pteropus poliocephalus* (PP, 928 g) were analysed by morphometric methods. These data increase fivefold the range of body masses for which bat lung data are available, and allow more representative allometric equations to be formulated for bats.

2. Lung volume ranged from 4.9 cm³ for PH to 39 cm³ for PP. The volume density of the lung parenchyma (i.e. the volume proportion of the parenchyma in the lung) ranged from 94% in PP to 89% in PH. Of the components of the parenchyma, the alveoli composed 89% and the blood capillaries about 5%.

3. The surface area of the alveoli exceeded that of the blood-gas (tissue) barrier and that of the capillary endothelium whereas the surface area of the red blood cells as well as that of the capillary endothelium was greater than that of the tissue barrier. PH had the thinnest tissue barrier (0.1204 μm) and PP had the thickest (0.3033 μm).

4. The body mass specific volume of the lung, that of the volume of pulmonary capillary blood, the surface area of the blood-gas (tissue) barrier, the diffusing capacity of the tissue barrier, and the total morphometric pulmonary diffusing capacity in PH all substantially exceeded the corresponding values of the pteropid species (i.e. PL, PA and PP). This conforms with the smaller body mass and hence higher unit mass oxygen consumption of PH, a feature reflected in the functionally superior gas exchange performance of its lungs.

5. Morphometrically, the lungs of different species of bats exhibit remarkable differences which cannot always be correlated with body mass, mode of flight and phylogeny. Conclusive explanations of these pulmonary structural disparities in different species of bats must await additional physiological and flight biomechanical studies.

6. While the slope, the scaling factor (b), of the allometric equation fitted to bat lung volume data ($b = 0.82$) exceeds the value for flight $\dot{V}_{O_{2max}}$ ($b = 0.70$), those for the surface area of the blood-gas (tissue) barrier ($b = 0.74$), the pulmonary capillary blood volume ($b = 0.74$), and the total morphometric lung diffusing capacity for oxygen ($b = 0.69$) all correspond closely to the $\dot{V}_{O_{2max}}$ value.

Phil. Trans. R. Soc. Lond. B (1991) **333**, 31–50

Printed in Great Britain

7. Allometric comparisons of the morphometric pulmonary parameters of bats, birds and non-flying mammals reveal that superiority of the bat lung over that of the non-flying mammal. However, the bat parameters relative to those of non-flying mammals deteriorate towards the higher body size range, because of the generally steeper slopes of the equations for non-flying mammals. Allometric comparisons also reveal that small-size bats have, in general, better adapted lungs than birds of equivalent size but at the higher body mass scale, bats are generally inferior to birds.

1. INTRODUCTION

Among the present day vertebrates, only bats and birds have mastered powered flight by solving the various biochemical, biophysical, and physiological problems associated with this form of animal locomotion. Because of their different evolutionary histories, different genetic resources and designs were utilized by these two groups to satisfy the demanding aerodynamic and energetic requirements of flapping flight. The maximal aerobic capacities ($V_{O_{2max}}$) of flying bats and birds are essentially the same, but are about two times greater than those of running mammals of similar size (see Thomas 1987). For this reason, bats provide a unique opportunity to explore the upper limits of design and performance in the mammalian respiratory system.

The pulmonary systems of mammals and birds are known to differ in several important ways (Hughes 1974, 1979; Maina 1985, 1986, 1989; Maina *et al.* 1989; McLelland 1989). Experiment evidence indicates that the through-flow avian lung with its cross-current pattern of gas exchange is functionally superior to that of the mammalian lung with its dead-end alveolar sacs and its uniform pool arrangement (Scheid & Piiper 1989; Powell & Scheid 1989). Nevertheless, bats with their mammalian lungs can exchange respiratory gases between the atmospheric air and their pulmonary blood during flight at rates similar to those of the seemingly highly adapted birds. Also, at least one species of bat (*Phyllostomus hastatus*) can maintain the same high lung oxygen extraction (E_L) values as a bird both during the metabolic stress of flight (Thomas *et al.* 1984) or when at rest during exposure to severe hypoxic stress (Farabaugh *et al.* 1985). Limited E_L values from larger sized bats, however, are considerably lower than corresponding data from *P. hastatus*, which suggests that the pulmonary performance of bats may be importantly influenced by body size (Thomas 1981; Thomas *et al.* 1985). In this regard, previous studies on some of the smaller bats have shown that the bat lung is morphometrically superior to that of a non-flying mammal, and that body size has an important influence on bat lung morphology (Maina *et al.* 1982; Maina & King 1984; Lechner 1985). Because pulmonary morphometric data are unavailable for any of the large sized bats, or for any species of bat for which $V_{O_{2max}}$ data are currently available, the relations between pulmonary structure and function in larger sized bats remain poorly understood.

This study examines quantitatively the pulmonary morphologies of four species of bats which include the microchiropteran species *Phyllostomus hastatus*, and

three of the larger megachiropteran species *Pteropus lylei*, *Pteropus alecto* and *Pteropus poliocephalus*. These species were chosen for both their body size, and the availability of some data for pulmonary function. The specific aims of this study were as follows.

1. Obtain for the first time lung morphometric data from some of the larger species of bats for which some relevant pulmonary function data are available in an attempt to better understand the relations between pulmonary structure and function in this unique group of mammals.

2. Use these additional data to formulate more representative allometric equations for bats so that we could more precisely assess the influence of body size on bat lung morphology and function, and,

3. Use these more representative bat allometric equations to compare key morphometric features of bat lungs with those of non-flying mammals and birds to appreciate the differences and similarities between these groups.

2. MATERIALS AND METHODS

The morphometric measurements were made on four specimens of *Phyllostomus hastatus* (PH), seven of *Pteropus lylei* (PL), one of *Pteropus alecto* (PA), and one of *Pteropus poliocephalus* (PP). The bats were killed by an intraperitoneal injection of euthatal and weighed. The trachea was isolated and cannulated. A small incision was made caudal to the xiphisternum, and the diaphragm carefully punctured on both sides of the mediastinum thoracis to create pneumothorax and a subsequent collapse of the lungs. The lungs were fixed by intratracheal instillation with 2.3% glutaraldehyde buffered in sodium cacodylate (pH 7.4, osmolarity 350 mOsm l⁻¹†) at a pressure head of 25 cm water above the supine body. After the fixative stopped flowing, the trachea was ligated and the lungs were left *in situ* for about 3 h before they were carefully removed after transecting the xiphisternum. A ligature was placed at the tracheal bifurcation and the trachea, the heart and the adhering tissues trimmed off. The lungs were subsequently immersed in fixative.

The various lobes of the lung were identified, and a ligature was placed on each lobar bronchus to retain the intrapulmonary fixative. The volumes of the individual lobes, and hence the total lung volume was determined by weight displacement method (Scherle 1970). Except for the middle lobe of the right lung which was set aside for airway dissection, each lobe of the lung was sampled by making transverse slices of about 1 cm thickness. Cranial, middle and caudal slices were taken from each lobe and individually diced

† One osmole contains one mole of osmotically active particles.

into small pieces (about 1 mm³) which were then processed for electron microscopy. The rest of the slices were processed for light microscopy.

(a) Light microscopy

The lung slices were either processed whole, where technically adequate, or were cut in half if they were too big. They were subsequently processed and embedded in paraffin wax using standard laboratory techniques. Serial transverse sections (7 µm) were cut and stained with haematoxylin and eosin. From each lobe, three equidistantly spaced sections were taken for analysis. The volume densities of the parenchyma and the non-parenchyma were determined on these stratified sections at a magnification of ×200 by point counting, using a quadratic lattice grid etched on a graticule and fixed to the eyepiece of the microscope. The absolute volumes of these main components of the lung were calculated from the total lung volume. The stereological (analytical) methods used have been described in detail in Weibel (1979*a*). Because the components of the parenchyma and non-parenchyma shrink in the same proportions (during tissue processing) the degree of shrinkage was not determined as the relative values of these parameters were used to determine their absolute values from the lung volume.

(b) Electron microscopy

The tissues for electron microscopy were post-fixed for 1 h in buffered osmium tetroxide (20 g l⁻¹) (pH 7.4), and then dehydrated in an ascending concentration of ethanol starting at 50% through to absolute and propylene oxide before infiltration and embedding in resin. Three blocks were picked from the three regions of each lobe of the lung. Ultrathin sections were cut, harvested on 200-square wiremesh grids and stained with lead citrate and uranyl acetate before viewing on a Zeiss EM 10 electron microscope. From each block, five electron micrographs were taken from the top right hand corner of consecutive grid squares (to avoid bias) at a primary magnification of ×1600. For each specimen, six micrographs were taken for analysis. In cases where the test area fell entirely in the alveolar space, such blanks were recorded and substituted in the final calculation. The negatives were enlarged by a factor of 3.5, and printed at a final magnification of ×5600 with a superimposed quadratic lattice grid. Point counting was employed to determine the volume densities of the components of the parenchyma; namely the alveoli, the blood capillaries, and the tissue of the interalveolar septum. The surface areas of the alveoli, the tissue barrier, the capillary endothelium, and the erythrocytes were determined by intersection counting. The area of the plasma layer was estimated as the mean of that of the capillary endothelium and the erythrocyte. The harmonic mean thickness (τ_{ht}) was determined by intercept length measurement along the grid lines using a logarithmic scale.

The morphometric pulmonary diffusing capacities (conductances) of the various components of the

air-haemoglobin pathway, namely that of the tissue barrier (D_{tO_2}), the plasma layer (D_{pO_2}) and the erythrocyte (D_{eO_2}), were determined using the physical coefficients for oxygen permeation of the tissue barrier (K_{tO_2}), the plasma layer (D_{pO_2}), and the coefficient for oxygen uptake by whole blood (Θ_{O_2}) which was adjusted using the venous haematocrits of each species. The membrane diffusing capacity for oxygen (D_{mO_2}) and the total morphometric pulmonary diffusing capacity (D_{LO_2m}) were calculated from the relevant individual serial conductances of the air-haemoglobin pathway. An appraisal of the model used in estimating these parameters is given in detail in Weibel (1970–71). The morphometric procedures and the physical constants used here are outlined in detail in Maina *et al.* (1989). Allometric equations of the pulmonary parameters of the eleven species, now available, were computed from individual (specimen) data points by least square minimization of variance on logarithmically transformed data. Similar equations were computed for birds reported in Maina (1989) and for non-flying mammals (see Gehr *et al.* 1981) on those species spanning comparable body mass range as the bats. The statistical comparison of the equations was performed using a SAS program package (SAS/STAT Guide for Personal Computers, Version 6, 1985: SAS Institute, Inc., pp. 773–876, 941–948).

3. RESULTS

The gross morphology of the lungs of PH, PL, PA and PP was similar. In these species the left lung was undivided, although in some specimens a shallow poorly defined notch was observed. The right lung consisted of cranial, middle, caudal and accessory lobes. The trachea and the bronchi were lined by ciliated cells intermixed with columnar non-ciliated cells (figure 6). The non-ciliated cells were characterized by abundant rough endoplasmic reticulum and scattered mitochondria. The general design of the lung was essentially similar to that reported for other species of bats in earlier studies (Maina *et al.* 1982; Maina & King 1984; Maina 1985, 1986). Basically, the lung consisted of the parenchyma and the non-parenchyma. The parenchyma comprised the alveoli, blood capillaries and the tissue of the interalveolar septum (figures 1–4) whereas the non-parenchyma was made up of the major air conducting passages (i.e. the bronchi up to and including the terminal bronchioles) and the blood vessels larger than capillaries. The interalveolar septum was sporadically perforated by the interalveolar pores (figures 1 and 3) and the blood capillaries bulged into the lumina of adjacent alveoli (figures 1 and 2).

The alveolar surface consisted essentially of squamous type I cells and rather cuboidal type II cells (figures 3 and 4). The type I cells (figure 4) had only a few organelles such as Golgi apparatus and mitochondria located at the perinuclear region, with cytoplasmic extensions that overlaid the alveolar surface (figure 5). The type II cells had an abundance of organelles including mitochondria, Golgi apparatus, rough and smooth endoplasmic reticulum and charac-

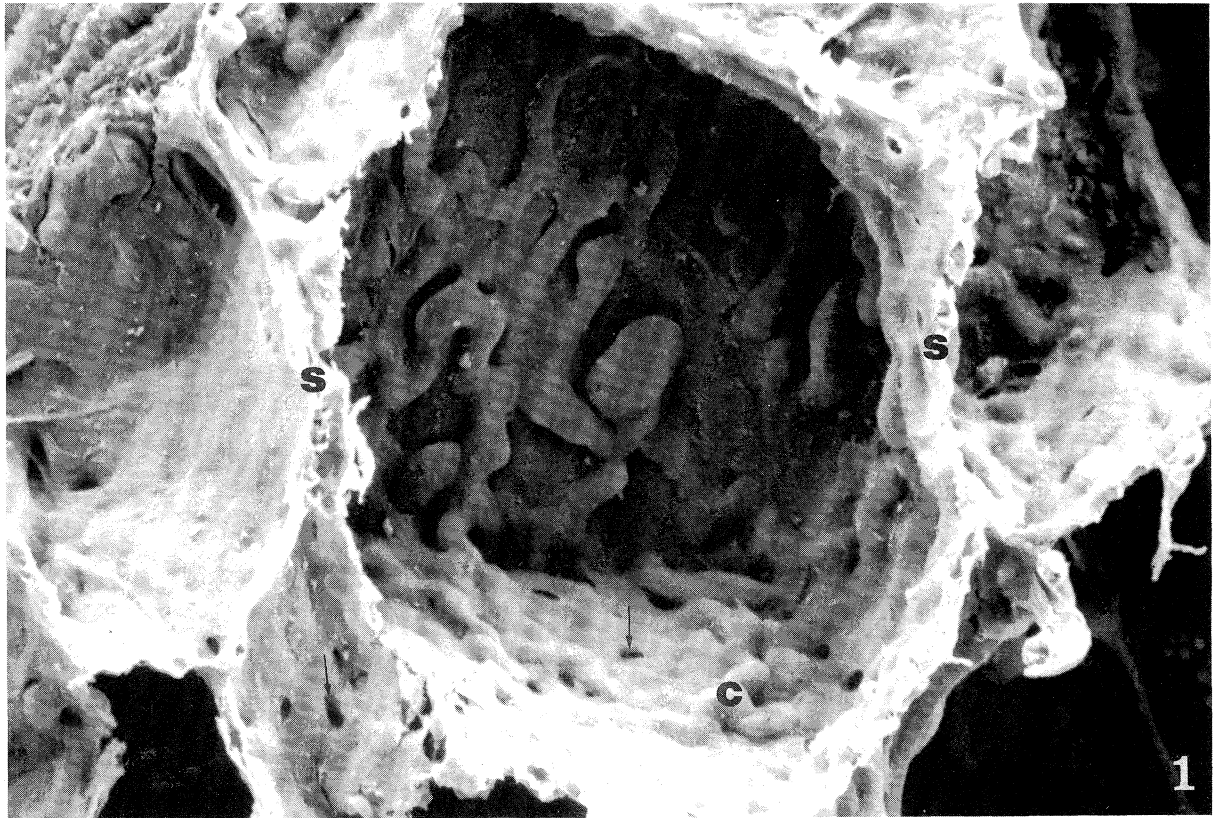


Figure 1. Scanning electron micrograph of alveoli, the terminal gas exchange components of the mammalian lung showing the dense capillary network (c) that lines the surface. s, Interalveolar septa perforated by the interalveolar pores (arrows). Magn $\times 1280$.

Figure 2. Scanning electron micrograph of the alveolar surface showing the dense capillary network. Arrows, type 1 cell junctions; s, interalveolar septum. Magn $\times 2180$.

teristically the lamellated osmiophilic bodies (figure 7). These cells had numerous stubby microvilli on the surface, and linked with the type I cells through distinct cell junctions. Occasionally, alveolar macrophages were observed on the alveolar surface or moving from one alveolus to another through the interalveolar pores (figure 4). The blood–gas (tissue) barrier consisted essentially of an endothelial cell and an epithelial cell with a common basal lamina (figure 5).

The morphometric results of this investigation are summarized in tables 1–8 and figures 9–17 inclusive, and show the following relations. The left lung composed 39% of the total lung volume in PH, 42% in PL, 47% in PA and 50% in PP (table 1). In the right lung, the caudal lobe was the largest, constituting 52% of the volume of the right lung in PH, 36% in PL, 44% in PA, and 46% in PP (table 1). The parenchyma constituted 88.5% of the lung in PH, 90.1% in PL, 88.1% in PA and 94% in PP (table 2). The alveoli composed the largest proportion of this part of the lung (table 3). In PH, the alveoli, blood capillaries, and the tissue of the interalveolar septum composed 89.5%, 5.8% and 4.7% of the parenchyma respectively, whereas similar values in PL were 88.5%, 4.9% and 6.6%, in PA 89.8%, 3.6% and 6.6% and PP 89.2%, 5.6% and 5.2%. In all the species investigated, the alveolar surface area exceeded both that of the blood–gas (tissue) barrier, and that of the capillary endothelium (table 4). The harmonic mean thickness of the blood–gas (tissue) barrier in PH (0.1204 μm) was smaller than that of PL (0.2092 μm) and PA (0.2849 μm), whereas PP had the thickest barrier (0.3033 μm) (table 4).

The oxygen diffusing capacities of the various components of the air–haemoglobin diffusion pathway are summarized in table 5. Because the physical constants for estimating the diffusing capacity of the plasma layer (K_{po_2}) and that of the red blood cells (Θ_{O_2}) are available as a range, these two parameters are given as minimum and maximum values. Because the reciprocal of conductance reflects resistance, it is apparent that the greatest resistance to oxygen diffusion along the air–haemoglobin pathway was associated with the erythrocytes where the conductance was lowest in all four species (table 5).

Some data normalized with body mass are presented in table 6, which show the following relations. The body-mass-specific volume of the lung (V_{L} m^{-1}) in PH (51 $\text{cm}^3 \text{kg}^{-1}$) was one and a half times that of PL (34) and PA (33), and about 1.3 times that for PP (42). The mass-specific surface area of the blood–gas (tissue) barrier (S_{t} m^{-1}) of PH (37 $\text{cm}^2 \text{g}^{-1}$) was greatest, whereas the mass-specific diffusing capacity of the tissue barrier ($D_{\text{tO}_2\text{m}}$ m^{-1}) of PH (1.2725 $\text{mlO}_2 \text{s}^{-1} \text{mbar}^{-1} \text{kg}^{-1}$) was four times that of PL (0.3043), six times greater than in PA (0.2177), and four times greater than in PP (0.2953).

Mass-specific total morphometric pulmonary diffusing capacity ($D_{\text{LO}_2\text{m}}$ m^{-1}) is the most comprehensive estimator of a lung's structural capacity for gas exchange. The ($D_{\text{LO}_2\text{m}}$ m^{-1}) value for PH (0.0663 $\text{mlO}_2 \text{s}^{-1} \text{mbar}^{-1} \text{kg}^{-1}$) was about twice that for PL (0.0312), four times that for PA (0.0158), and about one and a

half times that for PP (0.0478). This clear superiority of the $D_{\text{LO}_2\text{m}}$ of PH over those of the three pteropodid species results from the combination of (i) a more extensive body-mass-specific blood–gas (tissue) surface area, (ii) a notably thinner blood–gas (tissue) diffusion barrier, and (iii) a remarkably high body-mass-specific pulmonary capillary blood volume (table 6).

4. DISCUSSION

(a) Evolutionary background

Although mammals and birds both originated from cotylosaurian reptiles about 300 million years ago, the more recent progenitors of these two vertebrate groups branched from this lineage at different times. The birds evolved more recently from reptiles than did mammals (see Huxley 1868; Broom 1913; Heilmann 1926; Swinton 1960; Romer 1966; Ostrom 1973, 1975; de Beer 1975), thus explaining morphological similarities between extant birds and reptiles. Nevertheless, birds evidently evolved flight before the bats (Jepsen 1970), and presumably their early mastery of the diurnal niche exerted strong competitive pressures that forced bats into their nocturnal lifestyle. The study of flight is of interest as it illustrates the complex synergy of multiple factors like phylogenetic background, inherent morphological features and their malleability, and the constraints of mechanical design which an animal must confront as it adapts its various organ systems. The fact that bats and birds are the only extant vertebrates that are capable of powered flight attests to the extreme selective pressures during the course of their evolution.

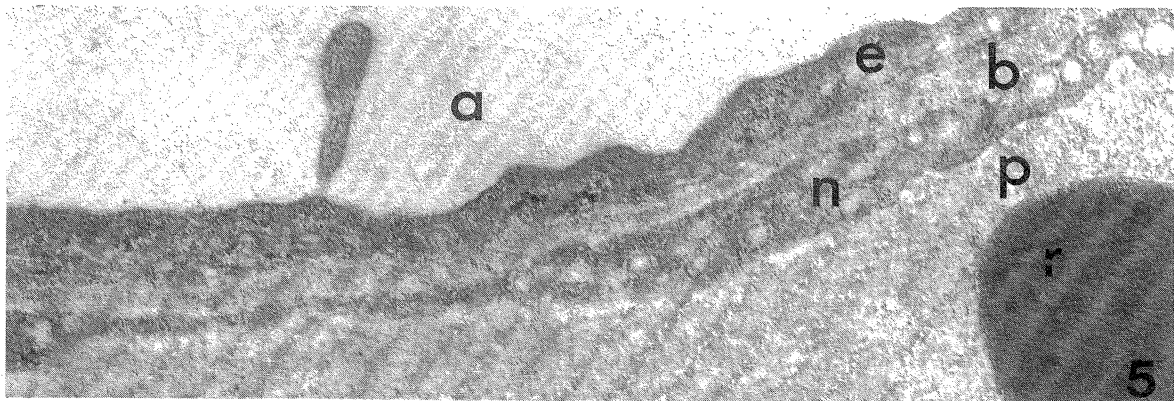
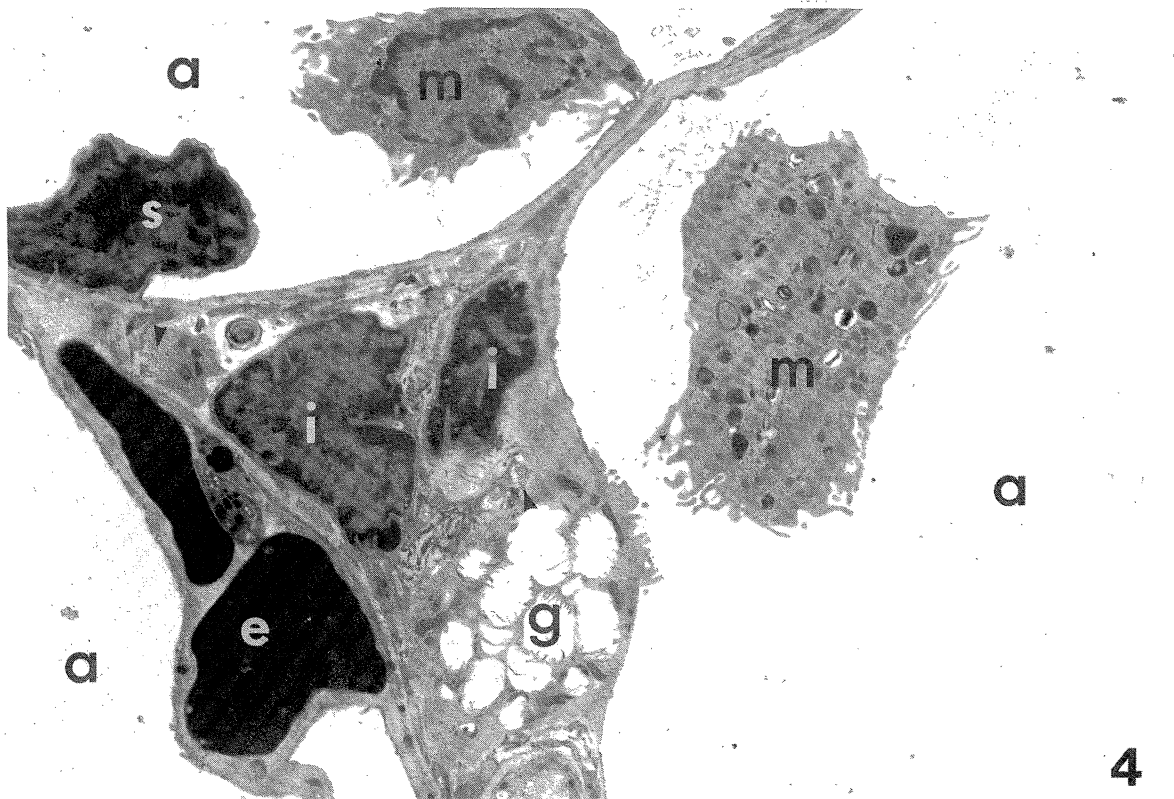
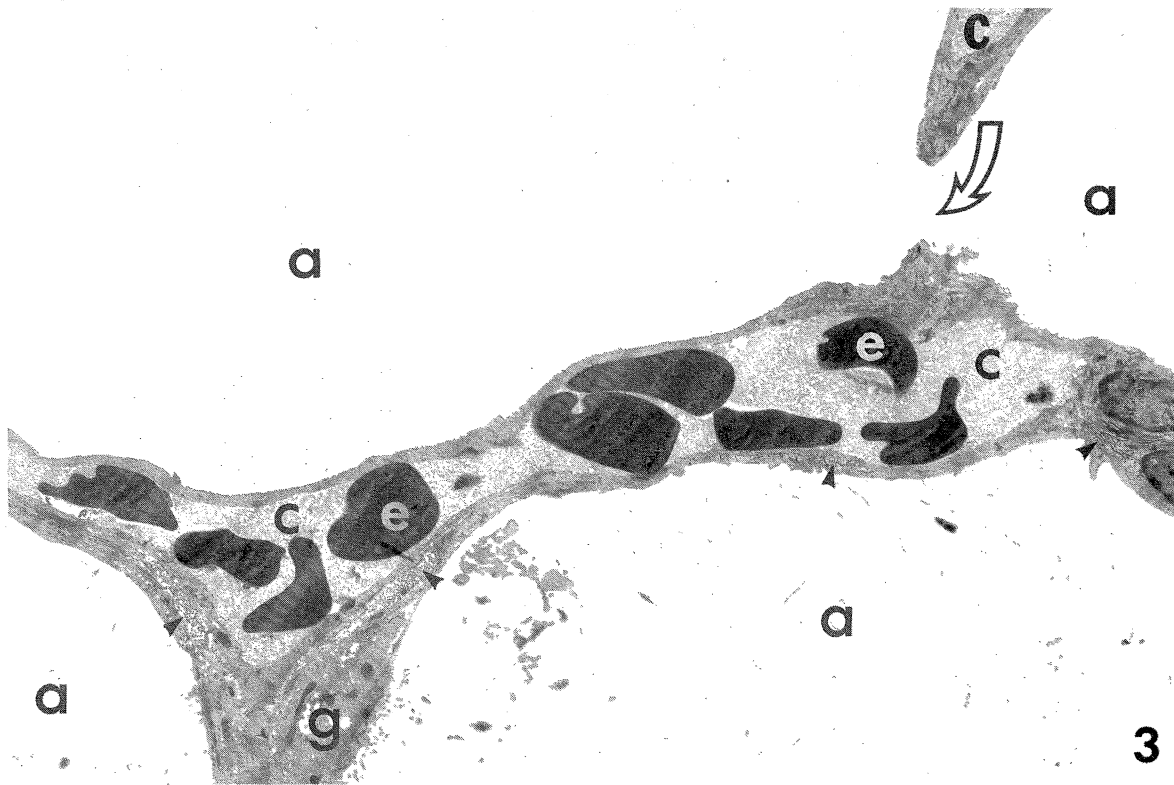
(b) Energetic requirements for flight

One prerequisite for flight that early bats and birds had to satisfy is its high metabolic requirement. Available data indicate that the maximal aerobic capacities ($V_{\text{O}_{2\text{max}}}$) of flying bats and birds of the same size are essentially the same, but range from 2.0 (when body mass = 100 g) to 1.6 (when body mass = 780 g) times greater than the $V_{\text{O}_{2\text{max}}}$ values from exercising non-flying mammals of the same size (figure 8). Moreover, extrapolations from existing data suggest that a 5 g bat may have a $V_{\text{O}_{2\text{max}}}$ which is 2.6 times that predicted for a non-flying mammal of this size. Even the minimal metabolic requirement of a bat or a bird in level flight is at least 1.5 times greater than the $V_{\text{O}_{2\text{max}}}$ capability of a non-flying mammal of the same size (Carpenter 1986; Thomas 1987). Thus a substantial difference in aerobic capacity distinguishes flying vertebrates from non-flying mammals.

(c) Morphological data of bat lungs and its relation to $V_{\text{O}_{2\text{max}}}$ and size

(i) Relations between bat lung structure, $V_{\text{O}_{2\text{max}}}$ and body mass

The present study extends the number of species of bats for which pulmonary morphometric data are available from 7 to 11, and expands the range of body sizes more than fivefold (table 7). These additional data have enabled the formulation of more rep-



Figures 3–5. For descriptions see opposite.

representative allometric equations for this group (table 8). Because structural design is the limiting factor for oxygen flow at each level of the respiratory system, and as body size is the single most important factor influencing the metabolic capacity of a flying bat (figure 8), allometric co-plots of $V_{O_{2\max}}$ and the various key lung morphological characteristics appropriately assess whether the size of the structures that influence oxygen flow are matched to functional needs of bats over a range of body sizes (figure 9a–f).

As expected, body mass has a very important influence on most lung morphometric parameters in bats, as it does in mammals generally (Weibel 1979b, 1984). As indicated by its steeper slopes, bat lung volume (V_L) increases more rapidly with increasing body mass than does $V_{O_{2\max}}$ (figure 9a). Calculations based on these relations predict that a 1000 g bat would have about 1.8 times the lung volume per unit of $V_{O_{2\max}}$ than a 10 g bat. Nevertheless, the $V_{O_{2\max}}$ specific surface area of the blood–gas (tissue) barrier (i.e. $S_t/V_{O_{2\max}}$) of bats is essentially independent of body mass, as indicated by the similar slopes of these two parameters (figure 9b), a relation that may reflect the higher surface:volume ratio of the smaller diameter alveoli of smaller-sized bats. Pulmonary capillary blood volume (V_c) and $V_{O_{2\max}}$ also scale similarly in bats (figure 9c), whereas harmonic mean thickness (τ_{ht}) is essentially independent of body mass (figure 9d).

As pointed out earlier, total morphometric pulmonary diffusing capacity (D_{LO_2m}) is the global estimator of a lung's structural capacity for gas exchange. As is apparent in figure 9e, D_{LO_2m} scales proportionally to $V_{O_{2\max}}$ in bats. Although we can not rule out the possibility that this correlation may be purely coincidental (e.g. because of other factors primarily, such as cardiac output and respiratory rate which are not directly and individually taken into consideration in a study such as this), it does suggest that bats are 'built reasonably' in that the dimensions of the respiratory systems of different size members of this group appear to be matched to their functional requirements. As will be elaborated upon below a somewhat different relation exists in non-flying mammals and birds.

At maximum exercise, where mismatch between ventilation and perfusion is reduced or even abolished, one would expect a lung's diffusing capacity for oxygen when measured by morphological methods, as in this study, i.e. D_{LO_2m} , to be numerically equal to its physiologically determined oxygen diffusing capacity, i.e. D_{LO_2p} ($D_{LO_2p} = V_{O_{2\max}}/p_AO_2 - p_CO_2$, where $(p_AO_2 - p_CO_2)$ is the alveolar to mean capillary pO_2

gradient in the lung). If this were the case, it would follow that the pO_2 gradient across the lungs of bats flying under $V_{O_{2\max}}$ conditions should also be essentially independent of body size, and have a predicted magnitude of about 73 Torr† (i.e. $(p_AO_2 - p_CO_2) = (V_{O_{2\max}}/D_{LO_2p})$) (figure 9f). Concerning the relation between D_{LO_2p} and D_{LO_2m} , unfortunately D_{LO_2p} data are unavailable for any species of bat. However, the assumption that, at $V_{O_{2\max}}$, D_{LO_2m} and D_{LO_2p} are the same appears not to be correct. In fact D_{LO_2p} never seems to equal D_{LO_2m} at least in man and the dog (Weibel 1984). The difference, though small, appears to be constant for a particular species. Weibel (1984) suggested that this could be explained by deficiencies in the techniques for determining D_{LO_2m} and D_{LO_2p} , and/or a safety margin such that morphologically the lung is somewhat overoptimized.

(ii) Deviations from allometric trends

Although the foregoing analyses show a close matching between the structure and function of bat lungs in general when viewed over a range of body masses (figure 9), individual species can show some prominent deviations from the trends. For example, the 37 g *Cynopterus brachyotes* has a body-mass-specific D_{LO_2m} (i.e. $D_{LO_2m} m^{-1}$) that is only about 60% of its allometrically predicted value (Maina & King 1984). Partly for this reason, this bat's $D_{LO_2m} m^{-1}$ is similar to that of the much larger PP (table 7). Interestingly, *Cynopterus* is incapable of hovering and has haematological parameters generally lower than those of a non-flying mammal of equivalent size (Snyder 1976). The morphometric features of the 96 g *Epomorphorus wahlbergi* are outstanding among the bats that have been examined so far (Maina *et al.* 1982). This fruit bat has enormous lungs, a remarkably extensive surface area of the blood–gas (tissue) barrier, and a large pulmonary capillary blood volume, features that culminate in its extremely high $D_{LO_2m} m^{-1}$ which is 1.7 times that of the considerably smaller *P. pipistrellus*, and 3.8 times greater than either the value allometrically predicted for a bat this size, or the value measured in the present study from the similar-size bat *P. hastatus* (table 7). *Epomorphorus* has an extensive foraging territory and is known to fly up to 500 km in one night (Fenton *et al.* 1985).

Among the bats investigated in the present study, the lungs of the intermediate-sized microchiropteran species *Phyllostomus hastatus* are morphometrically superior to those of the large-sized megachiropteran bats PL, PP and PA (table 6). Although this is expected † 1 Torr \approx 133.32 Pa.

Figure 3. Transmission electron micrograph of the exchange tissue showing alveoli (a) and blood capillaries (c). Arrow, interalveolar pore; g, type II (granular) pneumocyte; e, erythrocyte; arrow heads, collagen fibres of the interalveolar septa. Magn \times 7500.

Figure 4. A higher power view of the exchange tissue showing various cell types. m, Alveolar macrophages; s, type I (smooth) pneumocyte; g, type II (granular) pneumocyte; i, interstitial cells; e, erythrocyte; a, alveoli; arrow heads, collagen fibres. Magn \times 8000.

Figure 5. A high power view of the blood–gas (barrier) showing the alveolus (a), epithelial cell (e), basal lamina (b), and the endothelial cell (n). p, plasma layer; r, erythrocyte. Magn \times 88 000.

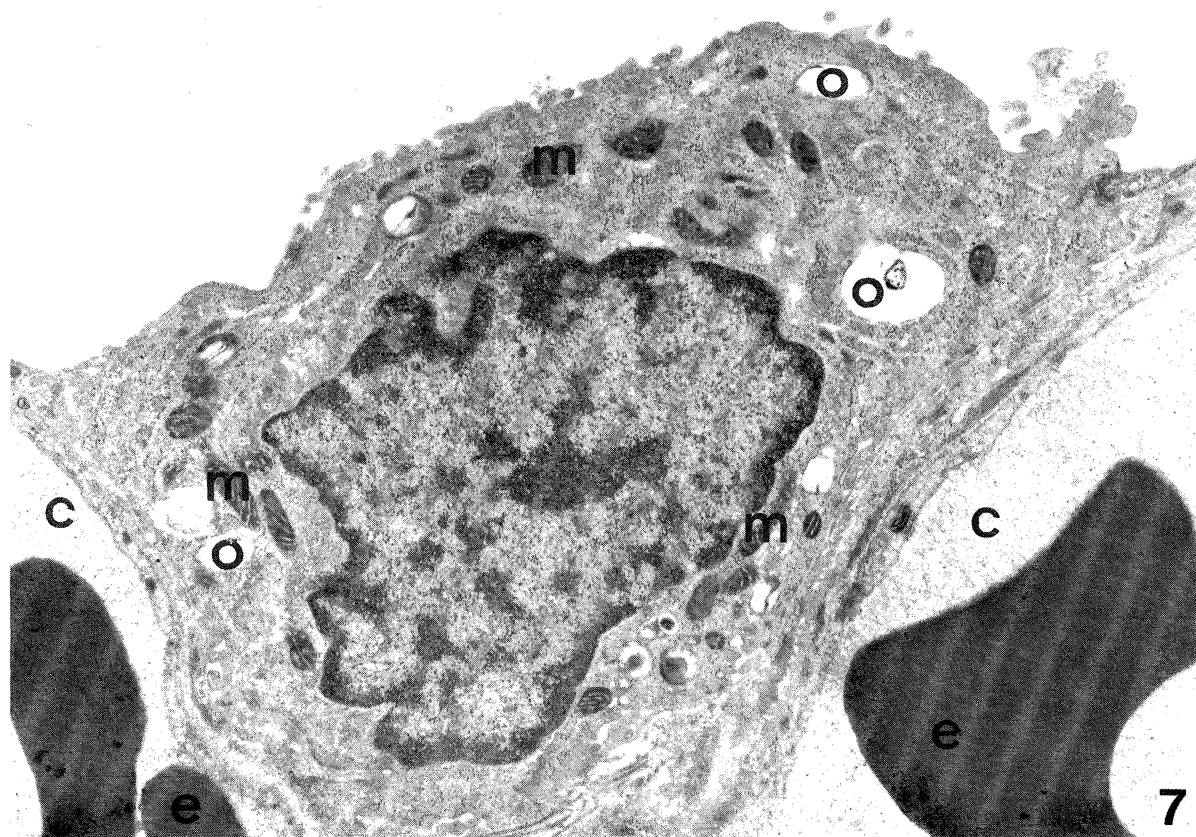
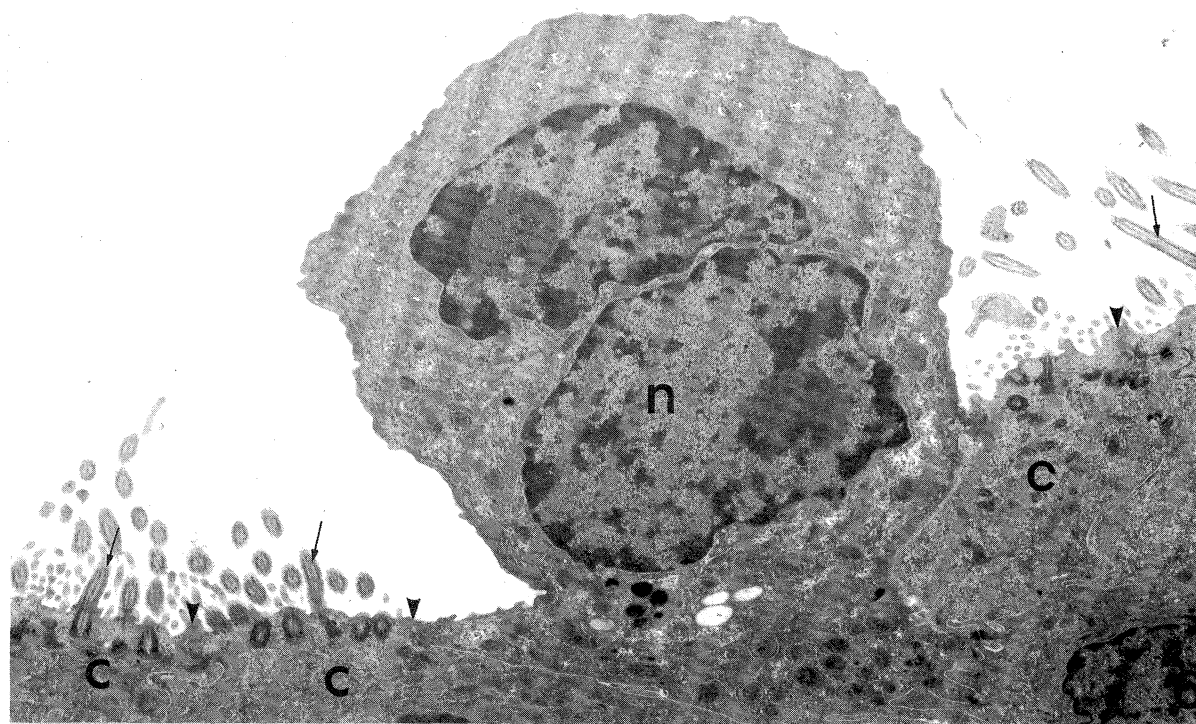


Figure 6. Transmission electron micrograph of non-ciliated (n) and ciliated cells (c) of the trachea. The non-ciliated cells have a bilobed nucleus and abundant rough endoplasmic reticulum. Arrows, cilia; arrow heads, cell junctions. Magn $\times 12000$.

Figure 7. A high power view of the type II (granular) pneumocyte. The osmiophilic lamellated bodies (o) precursors of the surfactant appear empty due to the fact that the material has been washed off during tissue processing. m, mitochondria; c, blood capillary; e, erythrocyte. Magn $\times 22090$.

Table 1. Individual lobe and total lung volume (cubic centimetres) of four species of bats

	left lung (undivided)	right lung				total volume
		cranial	middle	accessory	caudal	
<i>Phyllostomus hastatus</i>						
1	2.194	0.310	0.590	0.343	1.563	5.000
2	1.973	0.260	0.693	0.900	1.706	5.532
3	1.867	0.2867	0.550	0.783	1.633	5.120
4	1.660	0.350	0.530	0.210	1.380	4.130
mean ± s.e.	1.924	0.302	0.590	0.559	1.571	4.946
	0.096	0.017	0.031	0.145	0.061	0.255
<i>Pteropus lylei</i>						
1	4.647	1.394	1.586	0.609	1.563	10.550
2	4.365	1.1370	1.903	0.705	1.706	10.690
3	10.561	2.578	3.641	1.296	1.633	25.829
4	7.460	2.510	2.870	0.880	4.450	18.170
5	6.580	1.860	2.470	1.200	4.800	16.910
6	5.570	1.240	1.680	0.580	2.300	11.370
7	6.393	1.377	2.160	1.170	2.970	14.070
mean ± s.e.	6.511	1.728	2.330	0.920	2.775	15.370
	0.732	0.211	0.256	0.105	0.476	1.930
<i>Pteropus alecto</i>	10.419	1.776	3.615	1.159	5.234	22.203
<i>Pteropus poliocephalus</i>	19.764	3.387	5.124	1.941	9.019	39.235

Table 2. Volume densities (percent) and absolute volumes (cubic centimetres) of the parenchyma and non-parenchyma of the lungs of the fixed left and right lungs together in four species of bat of different sexes†

	sex	body mass/g	parenchyma		non-parenchyma	
			(%)	(cm ³)	(%)	(cm ³)
<i>Phyllostomus hastatus</i>						
1	M	94.9	86.25	4.313	13.75	0.688
2	M	105.0	89.90	4.973	10.10	0.559
3	M	91.5	86.75	4.442	13.25	0.678
4	?	100	91.110	3.763	8.891	0.367
mean ± s.e.		97.85	88.50	4.373	11.50	0.573
		2.56	1.03	0.215	1.03	0.065
<i>Pteropus lylei</i>						
1	M	466.0	85.86	9.058	14.14	1.492
2	M	501.6	93.10	9.953	6.90	0.738
3	M	558.0	89.56	23.132	10.44	2.697
4	M	377.0	91.66	16.660	8.34	1.515
5	?	412.0	91.60	15.490	8.40	1.420
6	?	438.8	89.99	10.232	10.01	1.138
7	?	438.8	93.78	13.195	6.22	0.875
mean ± s.e.		456.03	90.79	13.960	9.21	1.411
		20.87	0.93	1.740	0.93	0.225
<i>Pteropus alecto</i>	F	667.0	88.10	19.561	11.90	2.642
<i>Pteropus poliocephalus</i>	M	928.0	94.01	36.885	5.99	2.350

† ? The sex could not be conclusively determined.

because of the higher body-mass-specific $V_{O_{2max}}$ capabilities of this smaller-sized species, body mass alone does not account for all the diversity in this group. As several bat lung morphometric parameters tend to scale proportionally to $V_{O_{2max}}$ (figure 9), comparisons of actual versus allometrically predicted parameter values

(i.e. 'A:P ratios') provide a convenient way to quantify some of this interspecific diversity (table 9).

The close correspondence between actual and predicted $V_{O_{2max}}$ values (table 9) is not surprising, as PH, PA and PP comprise three of the five species used to generate the bat $V_{O_{2max}}$ allometric equations used in

Table 3. Volume densities (percent) and absolute volumes (cubic centimetres) of the main components of the parenchyma of the fixed left and right lungs together, namely the alveoli, blood capillaries and the tissue of the interalveolar septum in four species of bats

	alveoli		blood capillaries		septal tissue	
	(%)	(cm ³)	(%)	(cm ³)	(%)	(cm ³)
<i>Phyllostomus hastatus</i>						
1	89.540	3.862	4.842	0.209	5.618	0.242
2	92.751	4.613	4.146	0.206	3.103	0.154
3	88.959	3.952	6.722	0.299	4.319	0.194
4	86.620	3.260	7.480	0.281	5.900	0.222
mean ± s.e.	89.468	3.922	5.798	0.249	4.735	0.203
	1.094	0.240	0.677	0.021	0.558	0.017
<i>Pteropus lylei</i>						
1	88.519	8.018	3.593	0.325	7.888	0.714
2	86.514	8.611	5.448	0.542	8.038	0.800
3	91.386	21.139	5.445	1.260	3.169	0.733
4	92.750	15.448	2.260	0.376	4.990	0.831
5	83.890	9.181	8.530	0.934	7.780	0.830
6	89.270	13.433	3.710	0.558	7.020	1.056
7	87.350	11.526	5.620	0.742	7.030	0.928
mean ± s.e.	88.526	12.479	4.944	0.677	6.559	0.842
	1.045	1.637	0.705	0.116	0.636	0.041
<i>Pteropus alecto</i>	89.773	17.560	3.634	0.711	6.593	1.290
<i>Pteropus poliocephalus</i>	89.229	32.912	5.593	2.063	5.178	1.910

Table 4. Surface areas (square centimetres) of the structural components of the air-haemoglobin pathway and the harmonic mean thickness (micrometres) of the blood-gas (tissue) barrier and the plasma layer in four species of bats

(The values apply to both lungs together.)

	surface areas				thicknesses	
	tissue barrier	alveoli	capillary endothelium	red blood cells	tissue barrier	plasma layer
<i>Phyllostomus hastatus</i>						
1	3087.83	5737.39	3536.06	2619.68	0.1140	0.0828
2	3930.16	5323.29	3985.29	3715.39	0.1200	0.0996
3	3643.88	4676.93	3788.53	5200.12	0.1222	0.1180
4	3894.76	5412.61	4135.09	3336.11	0.1253	0.0817
mean ± s.e.	3639.15	5287.56	3861.24	3717.83	0.1204	0.0955
	168.45	192.37	112.20	470.96	0.002	0.007
<i>Pteropus lylei</i>						
1	1972.68	7327.99	3759.18	3441.21	0.1812	0.0770
2	6254.53	9633.49	7042.95	8171.33	0.1275	0.0595
3	10756.65	13716.80	10915.32	20257.33	0.1873	0.0668
4	5926.67	14130.67	6454.00	5016.67	0.2136	0.0569
5	9745.25	14700.31	11372.35	3562.27	0.3328	0.0761
6	5437.00	9873.73	5428.40	4132.92	0.2336	0.0713
7	7813.51	11361.75	8464.02	7229.53	0.1881	0.1092
mean ± s.e.	6843.76	11534.96	7633.75	7401.61	0.2092	0.0738
	1025.83	1276.46	979.92	2083.41	0.022	0.006
<i>Pteropus alecto</i>	10033.48	17311.25	10747.25	8369.21	0.2849	0.0904
<i>Pteropus poliocephalus</i>	20145.34	27443.12	21594.33	32692.20	0.3033	0.1367

this study. Except for its very low τ_{ht} value, the magnitude of the lung parameters measured from PH agree fairly well with their predicted values indicating that PH's pulmonary morphometry is typical for a bat of this size (table 9). The bats PL and PA in contrast

have S_t and V_c values that are substantially lower than their respective predicted values; characteristics which contribute to their lower-than-expected D_{LO_2m} values (table 9). Unlike PL, PA compounds its morphological disadvantages by having a greater than expected τ_{ht}

Table 5. Total anatomical pulmonary diffusing capacity (D_{LO_2}), the membrane diffusing capacity (D_{mO_2}) and the components of the air–haemoglobin pathway to oxygen, namely the tissue barrier (D_{tO_2}), the plasma layer (D_{pO_2}) and the erythrocyte (D_{eO_2}) in four species of bats

(Units: $\text{mlO}_2 \text{ s}^{-1} \text{ mbar}^{-1}$. The values apply to both lungs together.)

	venous haematocrit. (%)	D_{tO_2}	D_{pO_2}		D_{eO_2}		D_{mO_2}		D_{LO_2}	
			min	max	min	max	min	max	min	max
<i>Phyllostomus hastatus</i>										
1	65	0.1117	0.1488	0.2001	0.0034	0.0095	0.0638	0.0717	0.0032	0.0083
2	65	0.1351	0.1546	0.2080	0.0034	0.0093	0.0721	0.0819	0.0033	0.0084
3	65	0.1230	0.1523	0.2049	0.0048	0.1035	0.0680	0.0769	0.0045	0.0115
4	50.2	0.1282	0.2340	0.3148	0.0036	0.0098	0.0828	0.0911	0.0034	0.0089
mean \pm s.e.	61.6	0.1245	0.1724	0.2320	0.0038	0.0330	0.0717	0.0804	0.0036	0.0093
	3.2	0.004	0.018	0.024	0.001	0.020	0.004	0.004	0.0003	0.0007
<i>Pteropus lylei</i>										
1	44	0.0449	0.1870	0.2515	0.0049	0.0136	0.0362	0.0381	0.0043	0.010
2	44	0.2022	0.5116	0.6881	0.0082	0.0226	0.1449	0.1563	0.0078	0.0197
3	33	0.2367	0.9335	1.2556	0.0105	0.0290	0.1888	0.1992	0.0099	0.0253
4	46	0.1145	0.4032	0.5423	0.0044	0.0120	0.0892	0.0945	0.0042	0.0107
5	46	0.1208	0.3926	0.5280	0.0153	0.0423	0.0924	0.0983	0.0131	0.0492
6	46	0.0960	0.2682	0.3608	0.0044	0.0121	0.0707	0.0758	0.0043	0.0104
7	46	0.1714	0.2875	0.3867	0.0086	0.0237	0.1074	0.1188	0.0080	0.0198
mean \pm s.e.	43.6	0.1409	0.4262	0.5733	0.0080	0.0222	0.1042	0.1116	0.0074	0.0207
	1.7	0.023	0.87	0.117	0.001	0.004	0.017	0.019	0.001	0.005
<i>Pteropus alecto</i>	35	0.1452	0.4229	0.5688	0.0063	0.0173	0.1081	0.1157	0.0060	0.0151
<i>Pteropus poliocephalus</i>	45	0.2740	0.7942	1.068	0.0312	0.0860	0.2037	0.2181	0.0271	0.0617

Table 6. Mass specific lung volume ($V_L \text{ m}^{-1}$), surface area of the blood–gas (tissue) barrier ($S_t \text{ m}^{-1}$), volume of the pulmonary capillary blood ($V_c \text{ m}^{-1}$), pulmonary capillary haematocrit (H_c) and the diffusing capacities of the tissue barrier ($D_{tO_2} \text{ m}^{-1}$) and that of the whole lung ($D_{LO_2} \text{ m}^{-1}$) in four species of bat

(The values apply to both lungs together.)

	$V_L \text{ m}^{-1}$ ($\text{cm}^3 \text{ kg}^{-1}$)	$S_t \text{ m}^{-1}$ ($\text{cm}^2 \text{ g}^{-1}$)	$V_c \text{ m}^{-1}$ ($\text{cm}^3 \text{ kg}^{-1}$)	H_c (%)	$D_{tO_2} \text{ m}^{-1}$ ($\text{mlO}_2 \text{ s}^{-1} \text{ mbar}^{-1} \text{ kg}^{-1}$)	$D_{LO_2} \text{ m}^{-1} \dagger$ ($\text{mlO}_2 \text{ s}^{-1} \text{ mbar}^{-1} \text{ kg}^{-1}$)
<i>Phyllostomus hastatus</i>						
1	52.69	32.54	2.20	53.80	1.1770	0.0606
2	52.69	37.53	1.96	74.61	1.2867	0.0556
3	55.96	39.82	3.27	71.82	1.3443	0.0874
4	41.30	38.95	2.81	59.22	1.2820	0.0615
mean \pm s.e.	50.66	37.21	2.56	64.86	1.2725	0.0663
	2.98	1.41	0.26	4.31	0.030	0.006
<i>Pteropus lylei</i>						
1	22.64	4.23	0.697	71.82	0.964	0.0153
2	21.31	12.47	1.081	63.87	0.4031	0.0274
3	46.29	19.28	2.260	78.83	0.4242	0.0315
4	48.12	15.72	0.997	59.91	0.3037	0.0198
5	41.04	23.65	2.267	13.72	0.2932	0.0756
6	25.91	12.39	1.272	51.48	0.2188	0.0168
7	32.06	17.81	1.691	47.33	0.3905	0.0317
mean \pm s.e.	33.91	15.08	1.466	55.28	0.3043	0.0312
	3.94	2.17	0.218	7.48	0.041	0.007
<i>Pteropus alecto</i>	33.29	15.04	1.066	49.32	0.2177	0.0158
<i>Pteropus poliocephalus</i>	42.28	21.71	2.223	73.25	0.2953	0.478

† Mean of the maximum and minimum values.

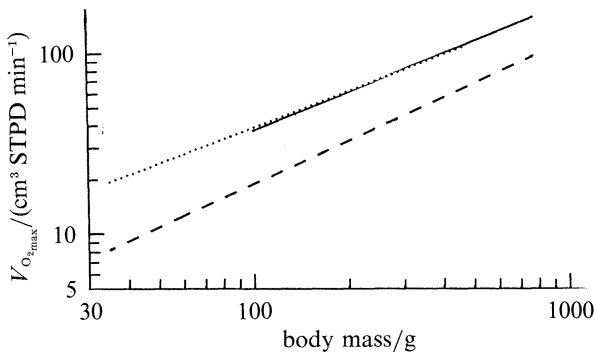


Figure 8. Comparisons of maximal aerobic capacities ($V_{O_{2max}}$) of bats (solid line), birds (dotted line) and non-flying mammals (dashed line). $V_{O_{2max}}$ values in bats are very comparable to those of birds, but exceed those of non-flying mammals by a factor of about 2. The data for bats are those of the species examined in this study, i.e. PH, PL, PA and PP whereas those of the birds and non-flying mammals were computed from $V_{O_{2max}}$ allometric equations for species within the mass range as the bats.

which further contributes to its extremely low D_{LO_2m} value. In contrast to these two pteropodid species, PP benefits from a slightly greater than expected S_t and a substantially greater V_c . Like PA, however, the lungs of PP are handicapped by a much greater than expected τ_{ht} (table 9). Despite its disadvantageous τ_{ht} , PP still manages to maintain a D_{LO_2m} that is much higher than that predicted for a bat of this size (table 9).

The ratio ($V_{O_{2max}}/D_{LO_2m}$) provides a morphometrically based estimate of the alveolar-to-capillary pO_2 gradient that may exist across the lungs of a flying bat. Although allometric analysis suggests that this gradient should be essentially independent of body mass in bats (figure 9e, f), the above variability in D_{LO_2m} results in a corresponding amount of interspecific variability in $V_{O_{2max}}/D_{LO_2m}$ (table 9). Particularly striking is the twofold difference in the morphometrically estimated

lung pO_2 gradients of PH and PA; a difference that suggests that compensating adjustments may exist in the respiratory physiologies of these two species.

As was mentioned earlier, one aim of this study was to obtain lung morphometric data from different species of bats for which some data for pulmonary function are available, to examine structure–function correlations. Lung oxygen extraction [$E_L = V_{O_2}/(\text{minute ventilation rate}, F_{I_{O_2}})$] is the fraction of the inspired oxygen that an animal's lungs remove for metabolic purposes, and provides a valid index for assessing the overall efficacy of the external gas exchange process. Although data for flight E_L are only available for two species of bats, the values for PH have been found to be about twice the corresponding values for PA (Thomas 1981; Thomas *et al.* 1984). Because available data indicate that the minute ventilation rates of flying bats are essentially independent of ambient temperature (Thomas 1987), these differences in E_L are probably not attributable to different levels of thermal hyperpnea in PH and PA, as can sometimes be the case for flying birds (Tucker 1968, 1972). Rather, these data suggest that the high V_{O_2} -specific minute ventilation requirements (i.e. low E_L) of PA relative to PH, may be a means by which the former bat enhances the diffusion gradient for respiratory gases across its lungs to compensate for their less advantageous morphological characteristics (table 9). Although this close intraspecific correspondence between D_{LO_2m} and E_L in PH and PA supports the thesis that structure and function are intimately related, one cannot completely dismiss the possibility that this close correspondence, like that between D_{LO_2m} and $V_{O_{2max}}$ (figure 9e), may simply be coincidental. E_L is a highly integrative parameter which is influenced by several factors, each of which can show compensatory shifts both within a given animal and from one species to another. Thus, in addition to the morphological disposition of the lung and factors that influence minute ventilation rate, E_L is influenced by factors such

Table 7. Comparison of pulmonary morphometric parameters in 11 species of bat

(The values apply to both lungs together.)

species	no.	body mass (g)	V_L m ⁻¹ (cm ³ kg ⁻¹)	S_t m ⁻¹ (cm ² g ⁻¹)	τ_{ht} (μm)	D_{tO_2} m ⁻¹ (mlO ₂ s ⁻¹ mbar ⁻¹ kg ⁻¹)	D_{LO_2} m ⁻¹
<i>Pipistrellus pipistrellus</i>	2	5.1	60.0	63.2	0.2060	1.27460	0.1471
<i>Pipistrellus subflavus</i>	6	5.4	44.71	61.1	0.2210	—	0.0795
<i>Mimopterus minor</i>	5	9.1	71.0	49.6	0.2160	0.9341	0.0962
<i>Tadarida mops</i>	5	24.0	97.0	56.1	0.2210	0.1073	0.1250
<i>Cynopterus brachyotes</i>	7	36.7	82.0	30.02	0.2820	0.4462	0.0511
<i>Epomophorus wahlbergi</i>	5	96.3	130	138	0.2670	2.3418	0.2500
<i>Phyllostomus hastatus</i>	4	97.85	50.66	37.21	0.1204	1.2725	0.0663
<i>Cheiromeles torquatus</i>	5	172.7	59	33.31	0.2020	0.6703	0.0521
<i>Pteropus lylei</i>	7	456.03	33.91	15.08	0.2092	0.3043	0.0312
<i>Pteropus alecto</i>	1	667	33.29	15.04	0.2849	0.2177	0.0158
<i>Pteropus poliocephalus</i>	1	928	42.28	21.71	0.3033	0.2953	0.0478

m, body mass; S_t , surface area of the blood–gas (tissue) barrier, V_L , volume of the lung; τ_{ht} , harmonic mean thickness of the tissue barrier; D_{tO_2} , diffusing capacity of the blood–gas (tissue) barrier to oxygen; D_{LO_2} , total anatomical diffusing capacity of the lung for oxygen.

Sources of data: *P. hastatus*, *P. lylei*, *P. alecto*, *P. poliocephalus*, this study; *P. pipistrellus*, *M. minor*, *T. mops*, *C. brachyotes*, *C. torquatus*, Maina & King (1984); *E. wahlbergi*, Maina *et al.* (1982); *P. subflavus*, Lechner (1985), mean values for the summer and winter bats.

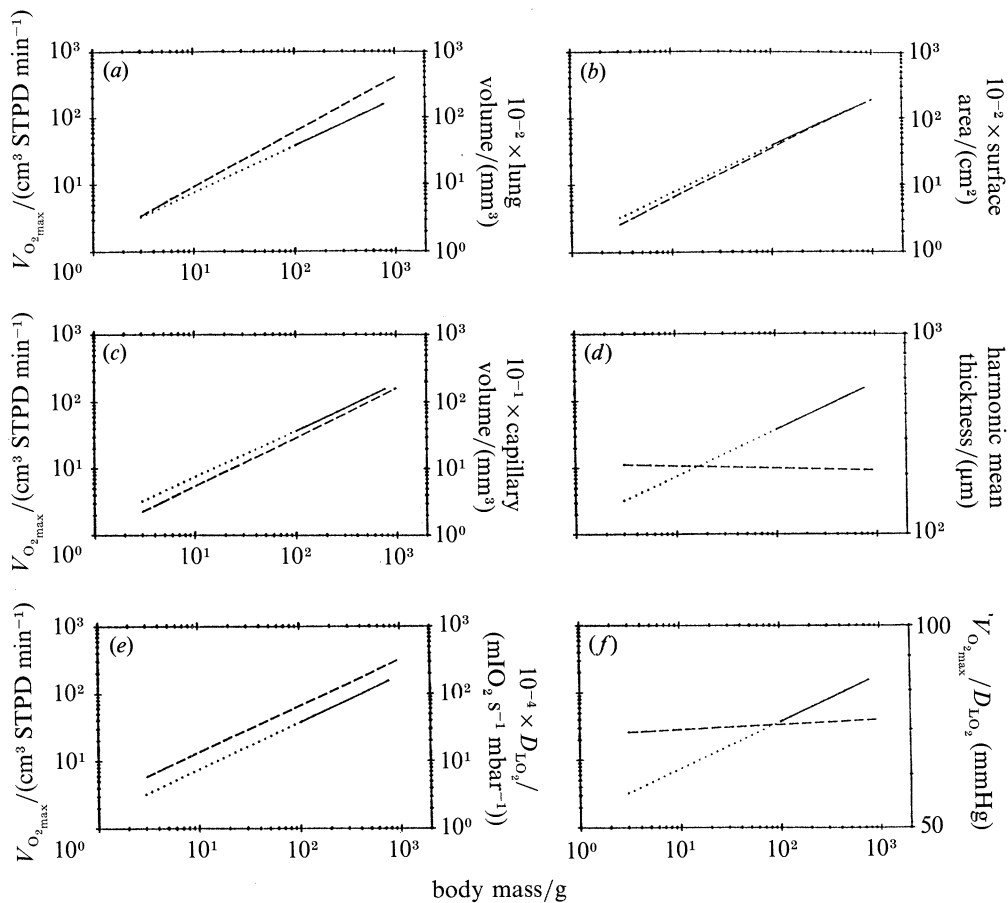


Figure 9. Allometric plots of flight ($V_{O_2_{\max}}$) (solid line with dotted line extrapolation beyond the data) and those of various bat pulmonary morphometric parameters (dashed line). (a) Lung volume increases faster with increasing body mass than $V_{O_2_{\max}}$ does. (b) The specific surface area normalized $V_{O_2_{\max}}$ of bats is almost independent of body mass as reflected in the comparable slopes of the two regression lines. (c) Pulmonary capillary blood volume and $V_{O_2_{\max}}$ also scale similarly for body mass. (d) Harmonic mean thickness of the blood–gas (tissue) barrier is independent of body mass indicating near optimization of this parameter. (e) The total morphometric pulmonary diffusing capacity scales proportionately with $V_{O_2_{\max}}$. (f) The morphometrically estimated alveolar pulmonary capillary p_cO_2 gradient ($= V_{O_2_{\max}}/D_{LO_2}$) is independent of body mass. The morphometric equations are based on those species of bats so far examined (table 7). The $V_{O_2_{\max}}$ equations are, however, based only on PH, PL, PA and PP (see equation 1 of Thomas (1987)).

Table 8. Allometric equations summarizing the relations between $V_{O_2_{\max}}$ or pulmonary morphometric parameters and body mass in bats

(The regression lines are expressed in the form $y = aw^b$, where y is the metabolic or pulmonary variable, a is the y -intercept, w is the body mass in grams, and b is the slope or the scaling factor. $V_{O_2_{\max}}$ equation is derived from equation 1 of Thomas (1987). Correlation coefficients (r) are also included. These regression equations are plotted in figure 9†.)

parameter	units	a	b	r	confidence intervals (b)	
$V_{O_2_{\max}}$	(M_{LO_2} STPD min^{-1})	1.48	0.700	0.95	0.678	0.723
V_L	(mm^3)	136.51	0.823	0.95	0.804	0.839
S_t	(cm^2)	113.80	0.738	0.87	0.732	0.744
V_c	(mm^3)	9.93	0.735	0.87	0.706	0.764
τ_{ht}	(nm)	225.32	-0.011	-0.06	-0.002	-0.020
D_{LO_2}	($\text{mlO}_2 \text{ s}^{-1} \text{ mbar}^{-1}$)	2.7×10^{-4}	0.692	0.84	0.659	0.724
$V_{O_2_{\max}}/D_{LO_2}$	(mmHg)	68.74	-0.0080	—	-0.0077	-0.0083

Definitions of symbols: $V_{O_2_{\max}}$, maximal steady state flight oxygen consumption; S_t , surface area of the blood–gas (tissue) barrier; V_c , pulmonary capillary blood volume; τ_{ht} , harmonic mean thickness of the blood–gas (tissue) barrier; D_{LO_2} , total morphometric pulmonary diffusing capacity for oxygen.

† The morphometric regression lines are based on the 11 species in which pulmonary data are presently available (table 7) while the $V_{O_2_{\max}}$ lines are on the four species investigated in this study namely PH, PA, PL and PP on which such data are available.

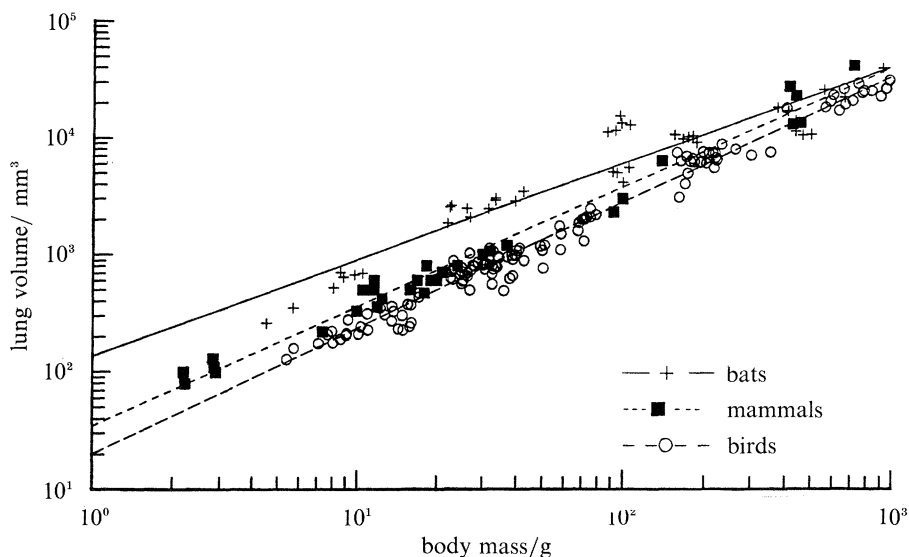


Figure 10. Allometric comparisons of the volume of the lung in bats, non-flying mammals and birds. In general the bats have larger specific lung volumes than non-flying mammals and birds. The convergence of the regression lines of the bats and non-flying mammals, however, suggests that the lung volume of a 1000 g bat may be similar to that of a non-flying mammal. The coefficients of the regression lines and the statistical comparisons for the pulmonary morphometric parameters in this figure, through to figure 16, are summarized in table 10. The regression line for the bats is based on the whole population (of bats) examined so far (table 7). That of the birds is derived from some of the species reported in Maina (1989) and Maina *et al.* (1989) within the same mass as the bats, and the non-flying mammals are from Gehr *et al.* (1981) similarly of comparable size range as the bats.

Table 9. Ratios of (measured: allometrically predicted) lung morphometric parameter values for the four species of bats investigated in the present study

parameter	PH	PL	PA	PP
$V_{O_2\max}$	1.08	1.00†	0.97	1.04
S_t	1.09	0.66	0.73	1.14
V_c	0.88	0.78	0.62	1.42
τ_{ht}	0.56	0.99	1.36	1.45
D_{LO_2}	1.00	0.75	0.44	1.45
$V_{O_2\max}/D_{LO_2}$	1.08	1.33	2.22	0.72

† Actual $V_{O_2\max}$ assumed to equal predicted value since no flight metabolic data are available for this species.

as the fraction of the inspired air that reaches the gas exchange regions of the lung, the ventilation: perfusion ratio of the lung, the respiratory properties of the blood, and the blood oxygen extraction abilities of the tissues. Unfortunately, most of these types of data are currently unavailable for bats.

(d) Allometric comparisons of bat, bird and non-flying mammal lung: morphological characteristics and their relations to $V_{O_2\max}$

(i) Significance of the comparisons

Because of the similar $V_{O_2\max}$ values of flying bats and birds, and the significantly lower values for non-flying mammals of equivalent size (figure 8), it is of interest to consider what similarities and differences exist in the pulmonary morphometric profiles of these different groups. Allometric comparisons of the regression lines of pulmonary parameters from the extended popu-

lation of bats (table 8) with those for non-flying mammals (Gehr *et al.* 1981) and birds (Maina 1989; Maina *et al.* 1989) have been made in figures 10–16. These are summarized in table 10 to find out whether more definite general conclusions beyond those made on a much more restricted population of bats (Maina & King 1984; Maina 1989) could be drawn concerning the relations between pulmonary structure and metabolic capability in these three vertebrate groups.

(ii) Allometric comparisons of bats with non-flying mammals

Comparisons of bats and non-flying mammals reveal that bats in general have notably larger lungs (figure 10). However, this difference diminishes as bats get bigger and at a body mass of about 1000 g the volume of the bat lung is essentially similar to that of a non-flying mammal. For example, on the lower scale of body mass, the mass-specific volume of the lung (V_L , m^{-1}) of the 5 g *Pipistrellus pipistrellus* is $60\text{ cm}^3\text{ kg}^{-1}$ (Maina & King 1984), whereas that of the shrew (*Crocidura juvenata*) with a comparable mass of 7 g (Gehr *et al.* 1981) is only $31\text{ cm}^3\text{ kg}^{-1}$. In the 456 g PL (this study), V_L m^{-1} is $34\text{ cm}^3\text{ kg}^{-1}$ and in a 441 g mongoose (*Helgale pervula*) (Gehr *et al.* 1981) the value of $32\text{ cm}^3\text{ kg}^{-1}$ is comparable. Similar trends in the allometric relations of bats and non-flying mammals are also apparent for the surface area of the blood-gas (tissue) barrier (figure 11) and the mass-specific surface area of the blood-gas (tissue) barrier (figure 12).

The volume of the pulmonary capillary blood (V_c) in bats is higher than that of the non-flying mammals only in bats below a body mass of about 70 g, above which non-flying mammals have a higher V_c (figure 13). Bats have a somewhat thinner blood-gas (tissue) barrier than non-flying mammals (figure 14). The

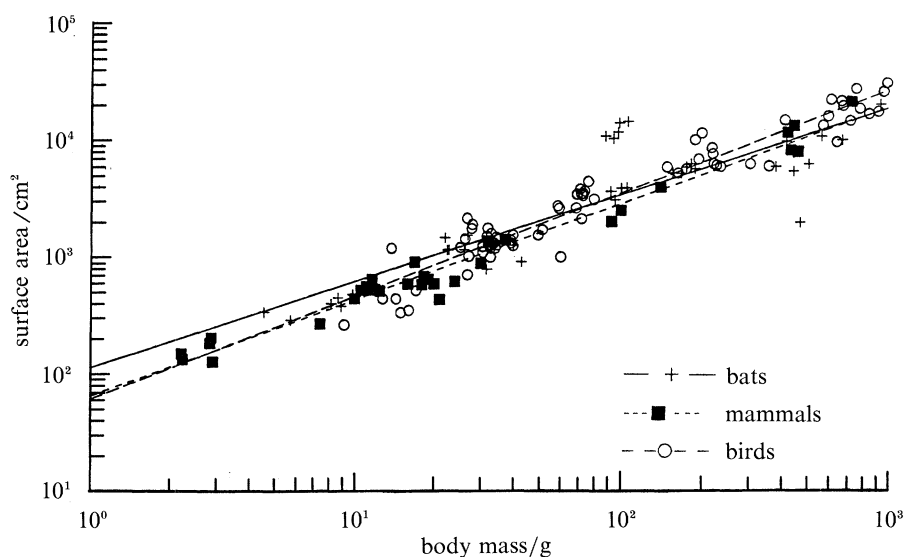


Figure 11. Comparison of the surface area of the blood-gas (tissue) barrier in the lungs of bats, non-flying mammals and birds. Smaller bats appear to have a more extensive surface area for gas exchange than the birds of equivalent body mass, whereas the value in the larger bats is less than that of the birds. Non-flying mammals in general have a smaller surface area than bats and birds. The convergence of the bat and non-flying mammal's regression line suggests a relative deterioration of this parameter in the heavier bats. For sources of data see figure 10.

Table 10. Allometric comparisons of some pulmonary morphometric parameters of bats, non-flying mammals and birds

(The regression lines are expressed in the form $y = aw^b$ where y is a pulmonary variable, a is the y -intercept, w is in grams, and b is the slope or the scaling factor. The correlation coefficient (r) and the probability levels (p) after statistical comparisons of the bats and the non-flying mammals (*), non-flying mammals and birds (+) and bats and birds (×) are given. A value of $p \leq 0.05$ was considered significant (SAS 1985). Plots of these regression lines are shown in the relevant figures 10–16.)

parameter	animal group	a	b	r	p
V_L	bats	136.51	0.8227	0.9481	s ($p \leq 0.001$)*
	mammals	34.69	1.0188	0.9904	s ($p \leq 0.001$) ⁺
	birds	13.67	1.0734	0.9896	s ($p \leq 0.001$) [×]
S_t	bats	113.80	0.7384	0.8733	n.s. ($p \geq 0.052$)*
	mammals	65.15	0.8219	0.9857	s ($p \leq 0.037$) ⁺
	birds	61.23	0.8800	0.9624	n.s. ($p \geq 0.957$) [×]
V_c	bats	9.93	0.7349	0.8745	n.s. ($p \geq 0.585$)*
	mammals	3.65	0.9762	0.9543	s ($p \leq 0.004$) ⁺
	birds	5.72	0.9377	0.9755	s ($p \leq 0.002$) [×]
τ_{ht}	bats	225.32	-0.0110	-0.0597	s ($p \leq 0.001$)*
	mammals	256.07	0.0752	0.6641	s ($p \leq 0.001$) ⁺
	birds	90.40	0.1074	0.5158	s ($p \leq 0.001$) [×]
D_{LO_2}	bats	2.7×10^{-4}	0.6924	0.8439	s ($p \leq 0.0001$)*
	mammals	6×10^{-5}	0.9181	0.9310	s ($p \leq 0.0001$) ⁺
	birds	1.4×10^{-4}	0.9022	0.9733	s ($p \leq 0.005$) [×]

Definition of the symbols and units: τ_{ht} , harmonic mean thickness of the blood-gas (tissue) barrier (nm); V_c , pulmonary capillary blood volume (mm^3); D_{LO_2} , total morphometric pulmonary diffusing capacity for oxygen ($\text{mlO}_2 \text{ s}^{-1} \text{ mbar}^{-1}$); V_L , volume of the lung (mm^3); S_t , surface area of the blood-gas (tissue) barrier (cm^2).

SAS/STAT guide for personal computers, version 6, 1985 (SAS Institute, Inc., pp. 773–876, 941–948).

thickness of this barrier, however, changes very little with body mass in both groups of mammals (figure 14). Weibel (1979*b*) has suggested that the thickness of the blood-gas (tissue) barrier in the lungs of the non-flying mammals has been optimized and genetically fixed during the course of their evolution. This also seems to be true for bats, at least in a statistical sense (figure 14).

From these relations, it is not surprising to find that the highly integrative D_{LO_2m} parameter scales less strongly to body mass in bats than it does in non-flying

mammals (table 10 and figure 15). These equations predict that although D_{LO_2m} should be about 2.7 times greater in a 10 g bat than in a non-flying mammal of the same mass, it should be essentially the same in 1000 g animals. We have previously shown that D_{LO_2p} and $V_{O_{2max}}$ scale proportionately in bats (figure 9*e*); data that supported the theme that bat lungs appear to be 'built reasonably'. In non-flying mammals, however, D_{LO_2m} (proportional to $W^{0.92}$) scales more strongly to body mass than does $V_{O_{2max}}$ (proportional to $W^{0.79}$)

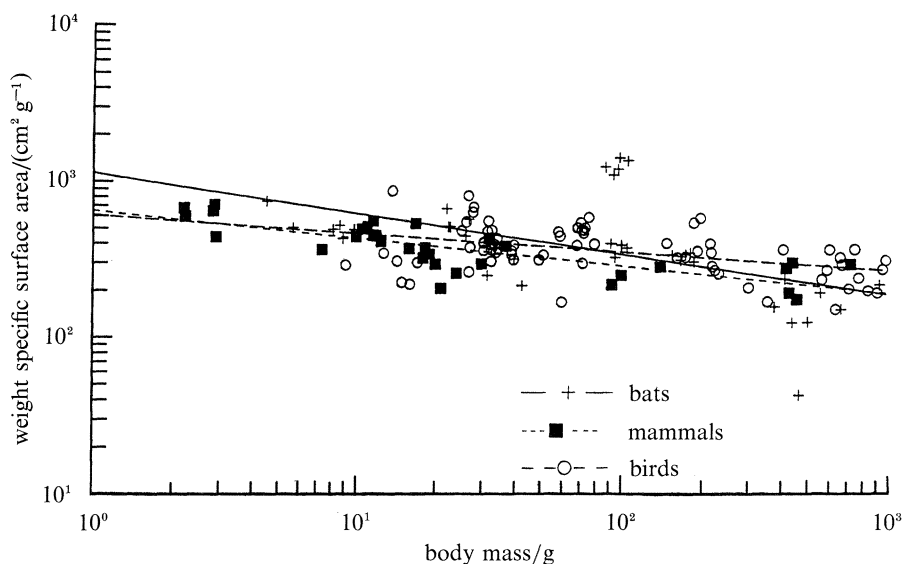


Figure 12. Comparison of mass specific surface area of the blood–gas (tissue) barrier against body mass. The negative slopes of the regression lines of the three groups of animals indicate that the size of the pulmonary structural parameters decreases in the larger and less metabolically active animals. The observations of the relations between the regression lines are similar to those made on figure 11. For sources of data see figure 10.

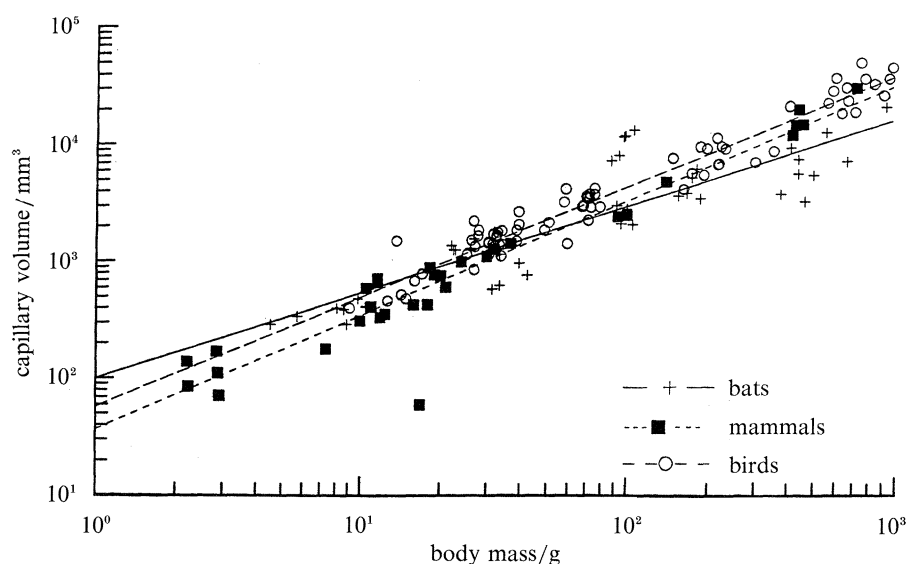


Figure 13. Comparison of the pulmonary capillary blood (V_c) in bats, non-flying mammals, and birds. Smaller bats have higher blood volumes than birds of similar size, whereas larger bats are inferior to the birds in this regard. Although the smaller bats have a higher V_c than the non-flying mammals, at higher body masses the volume is smaller in the bats. The birds in general have a higher V_c than the non-flying mammals. For sources of data see figure 10.

(Taylor *et al.* 1981). Does this mean that larger non-flying mammals have lungs which are ‘overdesigned’ in relation to their oxygen flow rates? Or does it mean that larger flying mammals have underdesigned lungs? Also, why should the D_{LO_2m} equation have a steeper slope than V_{O_2max} in non-flying mammals, but essentially the same slope as V_{O_2max} in flying bats despite the substantially higher metabolic capabilities of bats? If anything, one might intuitively expect this latter relation to be exactly opposite of what it appears to be.

Concerning the first question, Weibel *et al.* (1981) have attempted to explain the ‘apparent paradox’ between D_{LO_2m} and V_{O_2max} in non-flying mammals of different body sizes by pointing out that D_{LO_2m} is not the only factor determining oxygen flow from air to

blood in the lung. He suggests that there are reasons for suspecting that pO_2 gradient from alveolar air to capillary blood in non-flying mammalian lung may not be constant, but may be greater in smaller than in larger animals. Indeed, on the assumption that interspecifically morphometrically derived D_{LO_2} values parallel physiologically measured ones, allometric relations for non-flying mammals attest to this contention (figure 17). A large pO_2 gradient can result from either lowering p_{CO_2} (capillary oxygen partial pressure) or from elevating p_{AO_2} (alveolar oxygen partial pressure), or from both occurring simultaneously. Weibel has argued that this may be due to shorter blood transit times in the lungs of smaller animals (which would lower p_{CO_2}), or to better

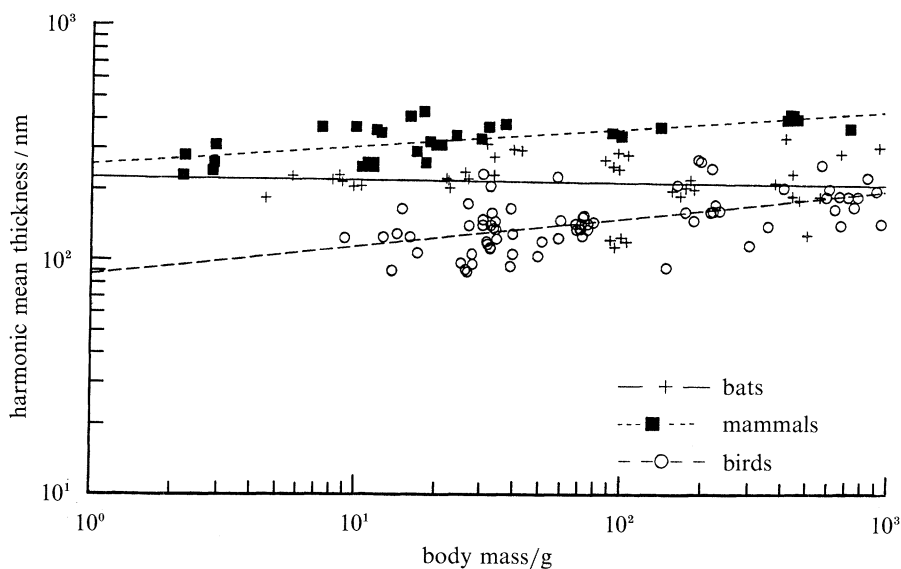


Figure 14. Comparison of the harmonic mean thickness of the blood-gas (tissue) barrier of the lungs of the bats, non-flying mammals, and the birds. The bats have blood-gas (tissue) barriers with thicknesses between those of birds (which have the thinnest barriers) and non-flying mammals. The convergence between the regression lines of bats and birds suggests that the magnitude of this parameter is comparable in the larger bats and birds. The almost zero slope in the bat regression line suggests optimization of this parameter in this taxon. For sources of data see figure 10.

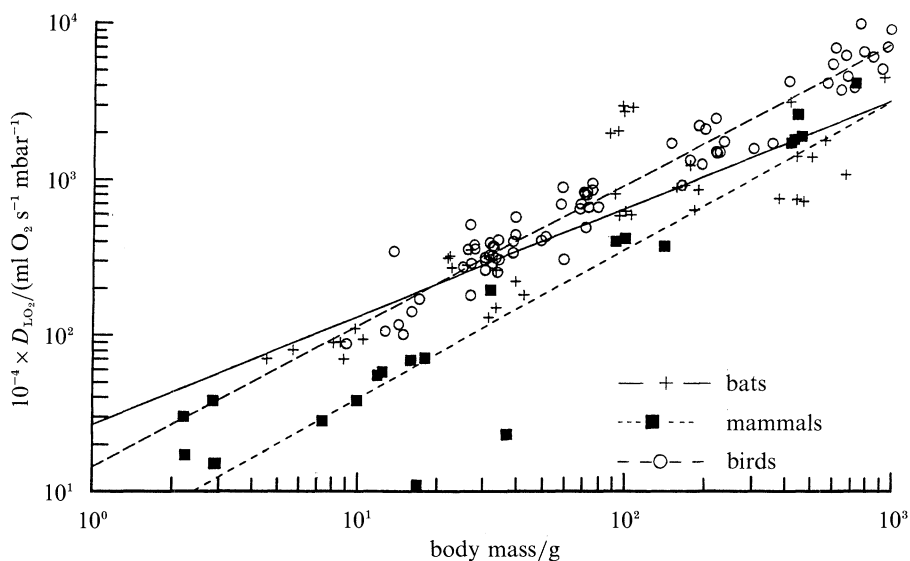


Figure 15. Comparison of the total anatomical pulmonary diffusing capacity (D_{LO_2m}) in bats, non-flying mammals and birds. Smaller bats have a higher D_{LO_2m} than birds, but quickly lose this advantage to the birds as body mass increases. In contrast to the significantly higher D_{LO_2m} values of small and intermediate size bats, the largest bats have D_{LO_2m} values comparable to those of non-flying mammals. Birds of all sizes have much higher D_{LO_2m} values than non-flying mammals of comparable size. For sources of data see figure 10.

alveolar ventilation in smaller species because they breathe at higher frequencies, or because of the effects of the acinus which is considerably smaller in small non-flying mammals and could result in a higher p_AO_2 (Weibel 1984). Concerning the aforementioned scaling differences between the lungs of bats and non-flying mammals, it is currently not possible to pinpoint the underlying reasons for these differences because of the almost complete lack of appropriate cardiorespiratory data from different size species of bats. One can only speculate that perhaps because exercising bats of all sizes maintain a 1:1 synchronization between their wing-beat and breathing cycles, they may be able to

ventilate their alveoli more effectively than can non-flying mammals as body mass increases, and thereby compensate for any underlying acinar size problems which accompany increasing body mass without having to overscale their lung morphometric parameters relative to V_{O_2max} .

The general convergence of the regression lines of the pulmonary parameters of the bats with those of the non-flying mammals, suggesting a relative deterioration of their pulmonary features, may explain the poor flight endurance in the larger bats (Carpenter 1986). On the other hand, the convergence admittedly may partly be due to lack of enough data particularly

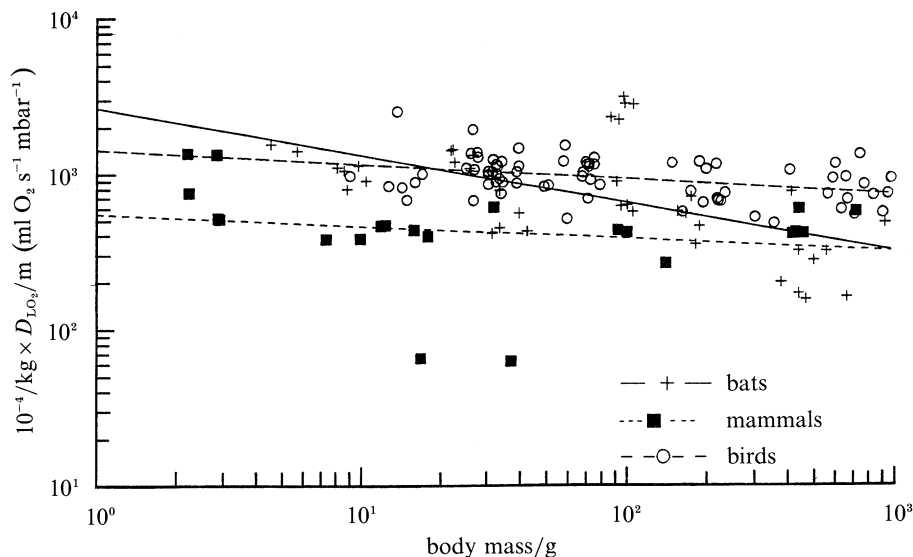


Figure 16. Comparison of mass specific total anatomical pulmonary diffusing capacity (D_{LO_2m} m^{-1}) in the bats, non-flying mammals and birds. The negative slope in the three groups of animals indicates a morphometric deterioration of the lungs in the larger species, and this is particularly true for bat lungs. The relations between the regression lines are similar to those outlined in figure 15. For sources of data see figure 10.

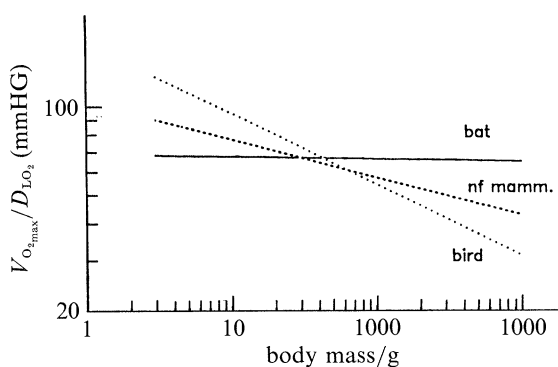


Figure 17. Comparison of the morphometrically estimated pO_2 gradient across the gas exchange components of the lung (V_{O_2max}/D_{LO_2} see text for details). This gradient is independent of body mass in bats, but drops off dramatically with increasing body mass in birds and the non-flying mammals. For sources of data see figure 10. V_{O_2max} values were generated from allometric equations for these taxa.

on bats. The mechanical requirements of flight are more favourable in the smaller bats (see Norberg & Rayner 1987) such species being more agile and manoeuvrable and even capable of hovering, the most energetically demanding form of flight (Weis-Fogh 1972; Epting 1980).

(iii) *Allometric comparisons of bats with birds*

Because of their similar metabolic capabilities and their very different pulmonary designs, birds provide a most interesting model to compare allometrically against bats. In a manner reminiscent of those described above, several parameters of bat lungs scale less strongly to body mass than do those of birds, so the relations between these two groups change with body mass. Thus, although small bats have larger lung volumes (figure 10) and thicker blood-gas (tissue) barriers (figure 14) than small birds, these differences all but disappear when body mass reaches 1000 g. The

surface area of the blood-gas (tissue) barrier (figures 11 and 12), the capillary blood volume (figure 13), and total anatomical pulmonary diffusing capacity (figures 15 and 16) are also higher in small bats than in small birds, but these relations are reversed as body mass exceeds a value of around 20 g such that a 1000 g bird would have a value about three times higher than that of a bat of similar size.

Concerning the latter observation, it is of interest to note that D_{LO_2m} (proportional to $W^{0.90}$, table 9) scales more strongly to body mass than does V_{LO_2max} (proportional to $W^{0.70}$) in birds, just as it does in non-flying mammals. Also apparent are the similar slopes of the allometric equations for D_{LO_2m} in birds and non-flying mammals (figure 15). Once again, what is the significance of these scaling differences? Do they mean that the design of the lung's diffusing capacity in birds and non-flying mammals is wasteful, and that bats are the only group with a more 'reasonable' design? Do they indicate that an overscaling to D_{LO_2m} relative to V_{O_2max} as body mass increases is the design standard for a vertebrate lung that is desirable to compensate for boundary condition breakdowns in the lung (e.g. V_A/Q inequalities), but for some reason bats have not conformed to this standard? Or, are these simply apparent differences that result from an inadequacy in the model used to calculate D_{LO_2m} values for the different groups from morphological data?

If one takes it that the morphometrically derived D_{LO_2} of a given animal group parallel their physiologically measured D_{LO_2p} values (i.e. $(p_A O_2 - p_C O_2) = (V_{O_2max}/D_{LO_2}) \dots$ see above discussion), allowing D_{LO_2m} to scale more strongly to body mass than V_{O_2max} would result in a predicted decline in the pO_2 gradient needed across the lung of an exercising bird or a non-flying mammal as body mass increases (figure 17). This contrasts with the prediction that the pO_2 gradient across a flying bat's lung may be independent of body mass (figures 9f and 17). Once again, we are unable to

pinpoint the underlying reason(s) for this difference because of the lack of appropriate physiological data from both groups, and the added complication of trying to compare two ventilatory systems of different design which may show different degrees of conformity to some of the assumptions one must make when performing a morphometric analysis such as this.

Finally with respect to the influence of body mass, aerodynamic theory predicts that the rise in an animal's mechanical power requirement for flight (P_{aero} , proportional to $W^{1.185}$) rises more steeply with increasing body mass than does its capacity for metabolic power production ($V_{\text{O}_2\text{max}}$, proportional to $W^{0.7}$) in both flying bats and birds. Therefore constraints on adaptation imposed by flight energetics should be stricter in larger bats and birds, and this particularly unfavourable scaling of P_{aero} to body mass should eventually impose an upper limit on the size that a flying animal can attain. In this regard, it is interesting to note that the largest bat (*Pteropus edulis*, 1380 g) weighs almost an order of magnitude less than the largest bird that is capable of steady flapping flight (the trumpeter swan, *Olor buccinator*, 12.5 kg (Calder 1974)). Carpenter (1986) observed that the larger bats have lower power reserves than the small ones. Although several alternative explanations are possible, it is tempting to speculate that the less favourable scaling of bat than bird pulmonary morphometric parameters to body mass might be an important reason why bats have not been able to evolve as great a body size as the largest flying bird.

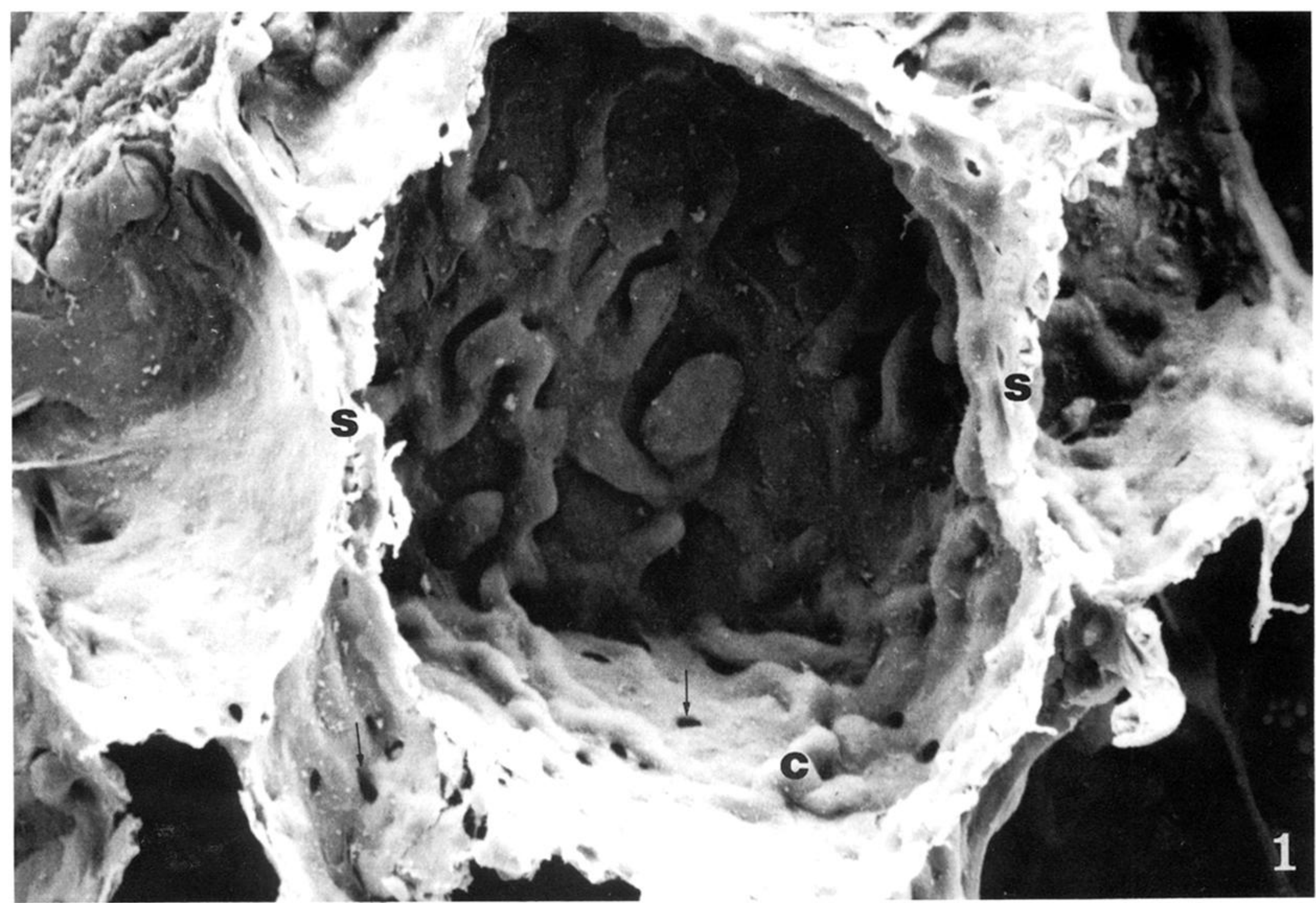
This collaborative research was made possible through a generous Fulbright Senior Scholar Fellowship awarded to J. N. Maina at University of California (Davis). J. N. Maina thanks Dr Dallas M. Hyde not only for his interest and active participation in this work but also for his hospitality and that of his staff during the tenure of the Fellowship. This work was partly supported by NSF Grant PCM-8303050 awarded to S. P. T.

REFERENCES

- Broom, R. 1913 On the South-African pseudosuchian Euparkelia and allied genera. *Proc. zool. Soc. Lond.* **1913**, 617–633.
- Calder, W. A. 1974 Consequence of body size for avian energetics. In *Avian energetics* (ed. R. A. Paynter), pp. 86–151. Cambridge, Massachusetts: Nuttall Ornithological Club.
- Carpenter, R. E. 1986 Flight physiology of flying foxes, *Pteropus poliocephalus*. *J. exp. Biol.* **114**, 619–647.
- de Beer, G. 1975 *The evolution of flying and flightless birds*. Oxford University Press.
- Epting, R. J. 1980 Functional dependence on the power for hovering on wing disc loading in humming birds. *Physiol. Zool.* **53**, 347–357.
- Farabaugh, A. T., Thomas, D. B. & Thomas, S. P. 1985 Ventilation and body temperature of the bat *Phyllostomus hastatus* during flight at different air temperatures. *The Physiologist* **28**, 272.
- Fenton, M. B., Brigham, R. M., Mills, A. M. & Rautenbach, I. L. 1985 The roosting and foraging areas of *Epomorphorus wahlbergi* (Pteropodida) and *Scotophilus viridis* (Vespertilionidae) in Kruger National Park, South Africa. *J. Mammal.* **66**, 461–468.
- Gehr, P., Mwangi, D. K., Amman, A., Maloiy, G. M. O., Taylor, C. R. & Weibel, E. R. 1981 Design of the mammalian respiratory system. V. Scaling morphometric pulmonary diffusing capacity to body mass: wild and domestic mammals. *Respir. Physiol.* **44**, 61–81.
- Heilmann, G. 1926 *The origin of birds*. London: Witherby.
- Hughes, G. M. 1974 *Comparative physiology of vertebrate respiration*, 2nd edn, pp. 68–70. London: Heinemann Educational Books.
- Hughes, G. M. 1979 *The vertebrate lung* (ed. J. J. Head), Carolina Biology Readers no. 59. North Carolina: Carolina Biological Supply.
- Huxley, T. H. 1868 On the animals which are most nearly intermediate between birds and reptiles. *Ann. Mag. nat. Hist. Ser.* **4**, 66–75.
- Jepsen, G. L. 1970 Bat organs and evolution. In *Biology of bats*, vol. 1 (ed. W. A. Wimsatt), pp. 1–64. London: Academic Press.
- Lechner, A. J. 1985 Pulmonary design in a micro-chiropteran bat *Pipistrellus pipistrellus* during hibernation. *Respir. Physiol.* **59**, 301–312.
- Maina, J. N. 1985 Scanning and transmission electron microscopic study of the bat lung. *J. Zool.* **205**, 19–27.
- Maina, J. N. 1986 The structural design of the bat lung. *Myotis* **24**, 71–76.
- Maina, J. N. 1989 The morphometry of the avian lung. In *Form and function in birds*, vol. IV (ed. A. S. King & J. McLelland), pp. 307–368. London: Academic Press.
- Maina, J. N. & King, A. S. 1984 Correlations between structure and function in the design of the bat lung: a morphometric study. *J. exp. Biol.* **111**, 43–61.
- Maina, J. N., King, A. S. & Settle, G. 1989 An allometric study of pulmonary morphometric parameters in birds, with mammalian comparisons. *Phil. Trans. R. Soc. Lond. B* **326**, 1–57.
- Maina, J. N., King, A. S. & King, D. Z. 1982 A morphometric analysis of the lung of a species of bat. *Respir. Physiol.* **50**, 1–11.
- McLelland, J. 1989 Anatomy of the lungs and air sacs. In *Form and function in birds*, vol. iv (ed. A. S. King & J. McLelland), pp. 221–279. London: Academic Press.
- Norberg, U. M. & Rayner, J. M. V. 1979 Ecology, morphology and flight in bats (Mammalia: Chiroptera): wing adaptations, flight performance, foraging strategy and echolocation. *Phil. Trans. R. Soc. Lond. B* **316**, 335–427.
- Ostrom, J. H. 1973 The ancestry of birds. *Nature, Lond.* **243**, 136.
- Ostrom, J. H. 1975 The origin of birds. *A. Rev. Earth planet. Sci.* **3**, 55–77.
- Powell, F. L. & Scheid, P. 1989 Physiology of gas exchange in the avian respiratory system. In *Form and function in birds*, vol. iv (ed. A. S. King & J. McLelland), pp. 393–437. London: Academic Press.
- Romer, A. S. 1966 *Vertebrate paleontology*, 3rd edn. University of Chicago Press.
- Scheid, P. & Piiper, J. 1989 Respiratory mechanics and air flow in birds. In *Form and function in birds*, vol. iv (ed. A. S. King & J. McLelland), pp. 369–391. London: Academic Press.
- Scherle, W. F. 1970 A simple method for volumetry of organs in quantitative stereology. *Microskopie* **26**, 57–60.
- Snyder, G. K. 1976 Respiratory characteristics of whole blood and selected aspects of circulatory physiology in the common shortnosed fruit bat *Cynopterus brachyotes*. *Respir. Physiol.* **28**, 239–247.
- Swinton, W. E. 1960 The origin of birds. In *Biology and comparative physiology of birds*, vol. 1 (ed. A. J. Marshall), pp. 1–13. London: Academic Press.
- Taylor, C. R., Maloiy, G. M. O., Weibel, E. R., Langman,

- V. A., Kamau, J. M. Z., Seeherman, H. J. & Heglund, N. C. 1981 Design of the mammalian respiratory system. III. Scaling maximum aerobic capacity to body mass: Wild and domestic mammals. *Respir. Physiol.* **44**, 25–37.
- Thomas, S. P. 1981 Ventilation and oxygen extraction in the bat *Pteropus gouldii* during rest and steady flight. *J. exp. Biol.* **94**, 231–250.
- Thomas, S. P. 1987 The physiology of bat flight. In *Recent advances in the study of bats* (ed. M. B. Fenton, P. Racey & J. M. V. Rayner), pp. 75–99. Cambridge University Press.
- Thomas, S. P., Lust, M. R. & van Riper, H. J. 1984 Ventilation and oxygen extraction in the bat *Phyllostomus hastatus* during rest and steady flight. *Physiol. Zool.* **57**, 237–250.
- Thomas, S. P., Thomas, D. B. & Thomas, G. S. 1985 Ventilation and oxygen extraction in the bat *Pteropus poliocephalus* acutely exposed to simulated altitudes from 0 to 11 km. *Fedn Proc. Fedn Am. Socs exp. Biol.* **44**, 1349.
- Tucker, V. 1968 Respiratory exchange and evaporative water loss in the flying budgerigar. *J. exp. Biol.* **48**, 67–87.
- Tucker, V. 1972 Respiration during flight in birds. *Respir. Physiol.* **14**, 75–82.
- Weibel, E. R. 1970–71 Morphometric estimation of pulmonary diffusion capacity, I. Model and method. *Respir. Physiol.* **11**, 54–75.
- Weibel, E. R. 1979a *Stereological methods: practical methods for biological morphometry*. London: Academic Press.
- Weibel, E. R. 1979b Oxygen demand and the size of respiratory structures in mammals. In *Evolution of respiratory processes: a comparative approach* (ed. S. C. Wood & C. Lenfant), pp. 289–346. New York: MerceL Dekker.
- Weibel, E. R. 1984 *The pathway for oxygen*. Cambridge, Massachusetts: Harvard University Press.
- Weibel, E. R., Taylor, C. R., Gehr, P., Hoppeler, H., Mathieu, O. & Maloiy, G. M. O. 1981 Design of the mammalian respiratory system. IX. Functional and structural limits for oxygen flow. *Respir. Physiol.* **44**, 151–164.
- Weis-Fogh, T. 1972 Energetics of hovering flight in hummingbirds and *Drosophila*. *J. exp. Biol.* **56**, 76–104.

Received 6 November 1990; revised 5 February 1991; accepted 18 March 1991



1

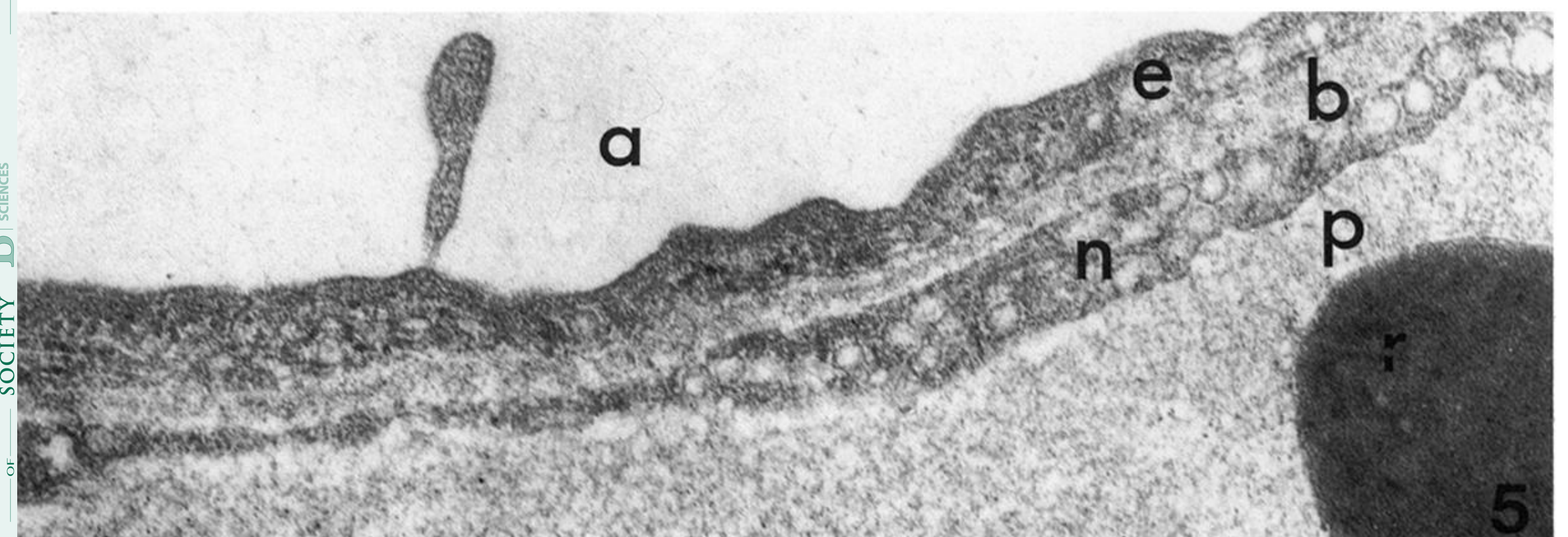
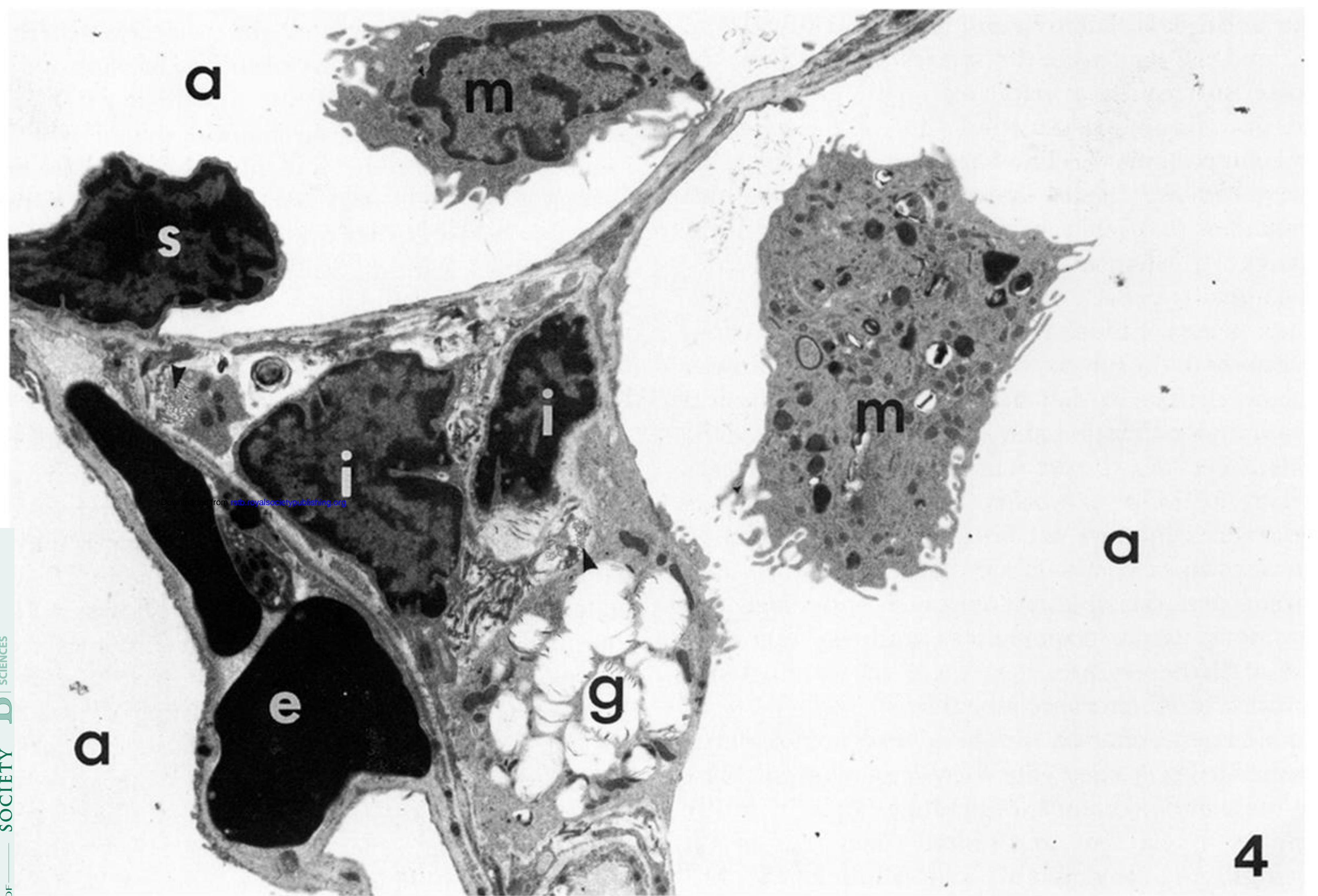
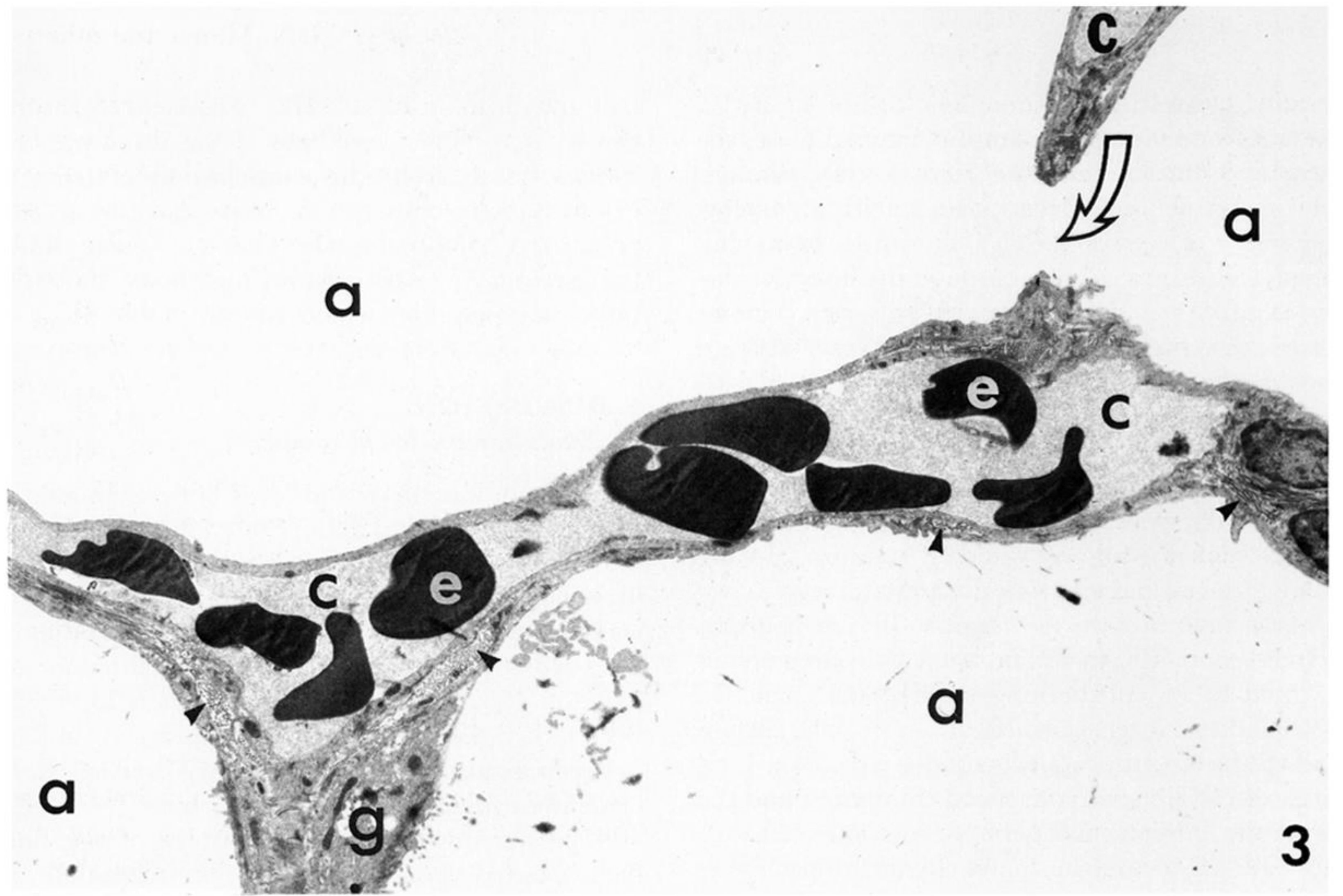


2

Downloaded from rsob.royalsocietypublishing.org

Figure 1. Scanning electron micrograph of alveoli, the terminal gas exchange components of the mammalian lung showing the dense capillary network (c) that lines the surface. s, Interalveolar septa perforated by the interalveolar pores (arrows). Magn $\times 1280$.

Figure 2. Scanning electron micrograph of the alveolar surface showing the dense capillary network. Arrows, type 1 cell junctions; s, interalveolar septum. Magn $\times 2180$.



Figures 3-5. For descriptions see opposite.

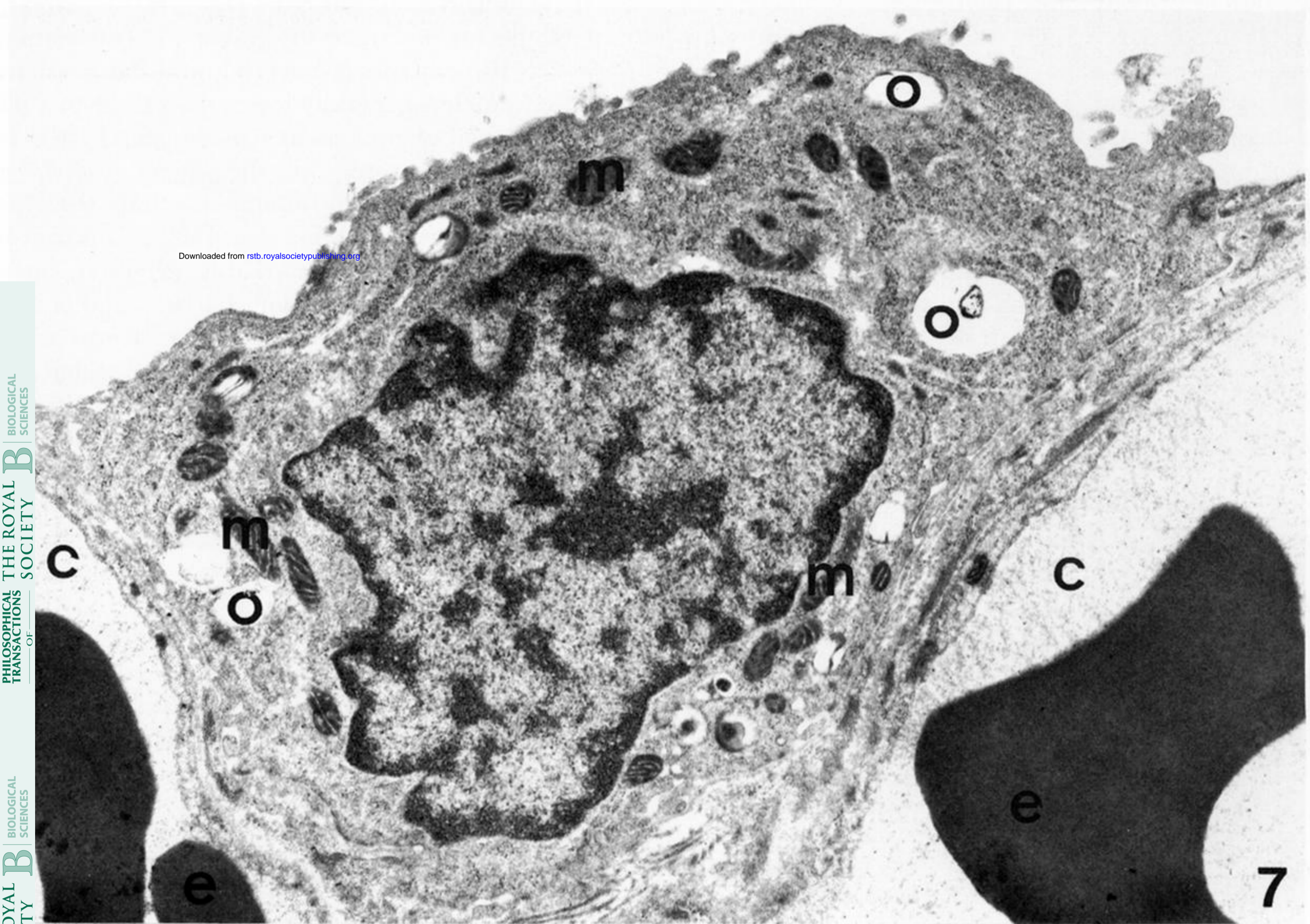
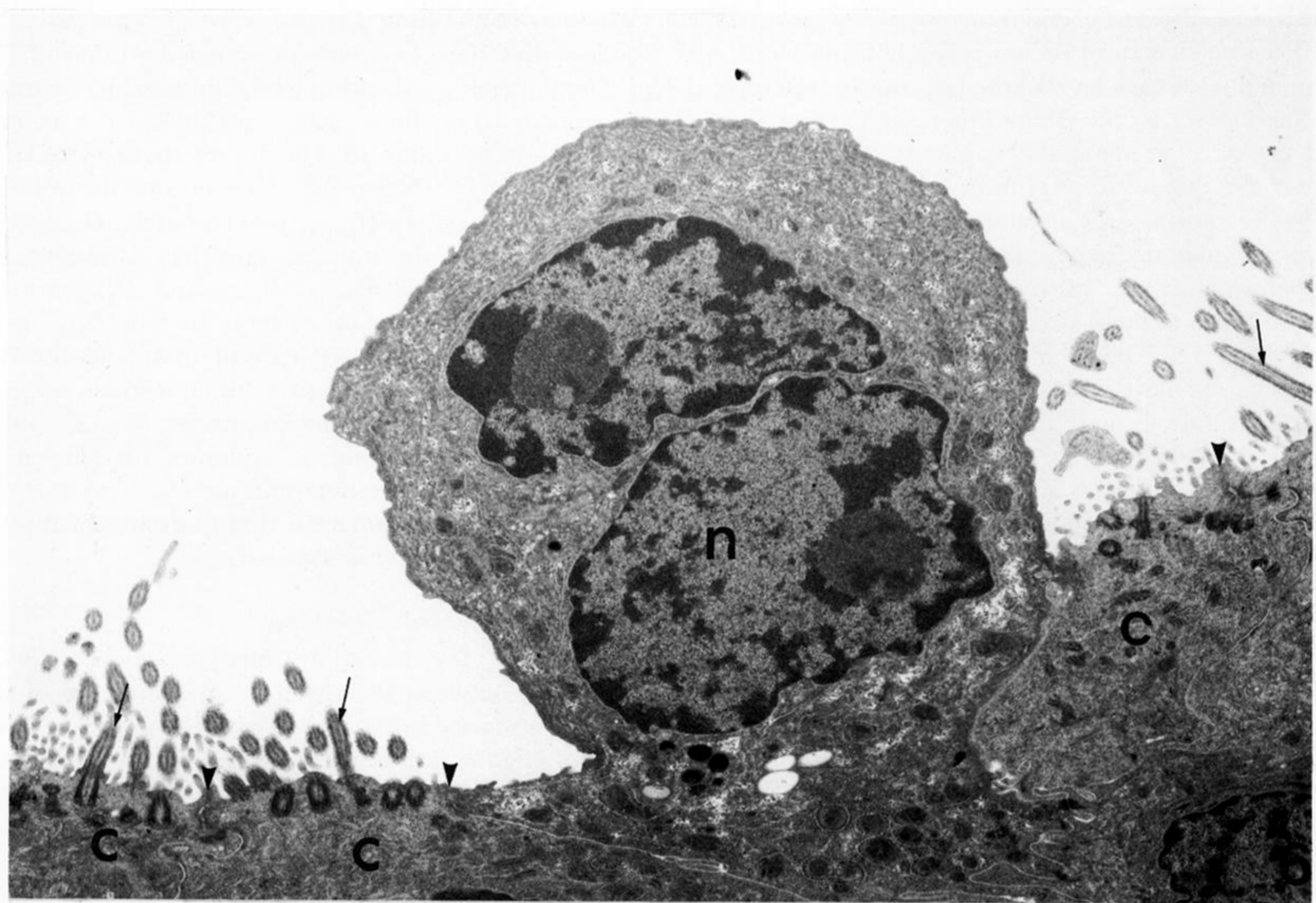


Figure 6. Transmission electron micrograph of non-ciliated (n) and ciliated cells (c) of the trachea. The non-ciliated cells have a bilobed nucleus and abundant rough endoplasmic reticulum. Arrows, cilia; arrow heads, cell junctions. Magn $\times 12000$.

Figure 7. A high power view of the type II (granular) pneumocyte. The osmiophilic lamellated bodies (o) precursors of the surfactant appear empty due to the fact that the material has been washed off during tissue processing. m, mitochondria; c, blood capillary; e, erythrocyte. Magn $\times 22090$.